ADDIS ABABA UNIVERSITY
COLLEGE OF NATURAL SCIENCES
SCHOOL OF EARTH SCIENCES

APPLICATION OF INTEGRATED GEOPHYSICAL TECHNIQUES FOR LANDSLIDE INVESTIGATION ALONG ARBAMINCH-GIDOLE ROAD IN DERASHE WOREDA, SNNP, ETHIOPIA

A thesis Submitted to the School of Graduate Studies

Addis Ababa University

In partial fulfillment of the requirements for the Degree of Masters in Exploration Geophysics

BY

KISANET ABERA

JUNE, 2016

Addis Ababa University

College of Natural and Computational Sciences

School of Earth Sciences

Geophysics Stream

APPLICATION OF INTEGRATED GEOPHYSICAL TECHNIQUES FOR LANDSLIDE INVESTIGSTION ALONG THE ARBAMINCH-GIDOLE ROAD IN DERASHE WORED, SNNP,ETHIOPIA.

By: Kisanet Abera

School of Earth Sciences

Approved by board of examiners:

Dr. Balemual Atnafu	_____	_____
Department Chairman	**Signature**	**Date**
Dr. Getnet Mewa	_____	_____
Advisor	**Signature**	**Date**
Dr. Abera Alemu	_____	_____
Internal Examiner	**Signature**	**Date**
Dr. Zemenu Geremew	_____	_____
External Examiner	**Signature**	**Date**

ABSTRACT

This research was conducted to assess the landslide problems occurred in Welaite Kebele located along the Arbaminch-Gidole Road, in Derashe Special Woreda, SNNP. The specific purposes were to determine the extent of the landslide affected zone, identify the triggering factors/ mechanisms, including mapping tectonic features. For these purposes Electrical Resistivity (with Vertical Electrical Sounding modification) and Magnetic methods of prospecting were utilized along specific lines.

From the survey results it has been possible to delineate three distinct lithological units with contrasting electrical properties. Accordingly, the top layer with variable resistivity (43-77 Oh-m) has a thickness range of 0-60m and it is associated with the response of colluvial deposit. The intermediate layer is highly conductive (2-32 Ohm-m) and relatively very thick (150-200 m) and attributed to the effect of a highly weathered and decomposed volcanic rocks which is well saturated. The substratum is marked by very high resistivity values (1400-10,000 Ohm-m) and it is delineated below the depth range of the second layer, i.e. 175-250m. Thus from these results the morphology of the major failure surface, which is between the contact of the second and the third layers, is clearly outlined. It shows a SE dipping trend with gentle dip angle -8.9^0. In addition, both the resistivity and magnetic survey data have equally suggested the possible presence of structurally disturbed zones around VES10, VES14, VES16, as well as VES4. These features are assumed to play their role in the process of mass sliding.

Based on the collected data analyses it became clear the road to Gidole is aligned over a deeply landslide affected zone, where along with the steeply dipping surface topography, the lithologic units are weak and highly saturated by groundwater and also affected by tectonics. Therefore, construction of road and other infrastructures require careful consideration of these real site conditions.

ACKNOWLEDGEMENT

Above all, I would like to thank “Almighty God” who made it possible to begin and finish this work successfully.

Foremost I am grateful to my advisors Dr.Getnet Mewa for his help during data processes, fatherly approaches, encouragements, constructive comments, and suggestions throughout the research work. Thank you very much Dr.Getnet Mewa for your unforgettable help you did during all the ups and downs of my work.

I would like to thank to Prof.Tigistu Haile, Prof. Tilahun Mammo and Dr. Abera Alemu to give me a detailed well summarized theoretical background of the subject matter.

I am indebted to Teklebrhan Ambaye Construction (TACON) for supporting me financially. I extend my gratitude to Addis Ababa University (AAU) particularly IGSSA for letting me collect the data from the study area along with them. Additionally I extend thanks to Dr.Genet Tamiru and Ato.Gtachew Abrha (from IGSSA, AAU) for their assisting and cooperation during primary data collection and processing that leads to achieve my research work properly.

Special appreciations go to Adiss Eshetu and Geremew Lamessa for their help in various software and geophysical explanations of the thesis. It gives me a special privilege to extend my deep thanks to all my friends.

Last but not least, I sincerely thank to all my beloved family for their love and encouragement. I do not have words to thank particularly my mother Mulu and my fiance Mekonnen for their treatments and bases for my success.

Table of content

Table of Content

Acronyms

DEM - Digital elevation model

EC - Electrical Conductivity

EGS - Ethiopian Geological Sur

GPS - Global position system

Jr - Intensity of remnant magnetization

IGRF - International Geomagnetic Reference Field

masl - meters above mean sea level

VES - Vertical Electrical Soundings

nT - nanoTesla

Am - Ampere per meter

NS - North-South

NE - North-East

SW - South-West

DP - Damage Potential

CHAPTER –1

1. INTRODUCTION

1.1 Background

The unique tectonic setting and accompanying active rifting processes have exposed Ethiopia for seismic and volcanic risks. Besides, its complex geological and geo-morphological features, coupled with the continuously deteriorating environmental conditions, have made most parts of the country vulnerable for landslide and related risks and often damage built infrastructures and natural environment. Every year Ethiopia allocates a significant amount of budget for the expansion of road network to facilitate movements of people and commodities that ultimately contribute for the economic progress. Nowadays, Ethiopia has many existing and under construction main roads which are used to connect different parts of the country and the country to the neighboring countries. Its development plan envisages construction of new and also upgrading of the existing roads so as to provide better transportation access to urban and rural communities. Eventually this enables them to play significant role in the economic transformation, and the national development in general.

Despite these efforts, from time to time the rates and intensities of damages of built infrastructures and natural environment caused by landslides and related geo hazard phenomena is rising significantly. Today landslide has become one of the major threats to people, property, including built structures such as roads, bridges, houses, dam reservoirs, communal properties (schools, health centers, sport fields, etc), fertile farmlands, parks and forests, etc. Sizes of the sliding masses vary from few meters to hundreds of millions of cubic meters masses and detachment of such masses of volumes have considerable impact in changing the shape of the earth's surface.

Globally, only in the 20th century the International Landslide Centre (ILC) has estimated the number of fatalities to be over half-million and the economic lose by landslides exceeds $10 billion annually (Steffen Hagedorn, 2014). However, advancements in technologies and researches have contributed to better understanding of the processes involved in the landslides

and under favorable conditions provide opportunities to forecast them, and thus minimize their economical, social and environmental impacts.

The term landslide is defined as movement of wide range of soil/rock masses down slopes or cliffs under the influence of gravitational force. The phenomena can take place on any type of rock / soil suddenly or slowly over long period of time. Based on the types of movements and nature of sliding materials, mass movements can be classified as rock/soil falls, topples, slides, flows and spreads or any mixture of these (Varnes, 1978; Crude and Varnes, 1996). A number of mapping procedures for landslides have been developed to identify and characterize unstable areas and adopt suitable preventive measures (Varnes (1984). In order to provide a systematic approach to study landslides, Anbalagan and Singh (1996) explained such theoretical concepts as danger, hazard and risk.

Danger refers to an existing natural phenomenon, such as creep, rock fall or debris slide. The danger can be an existing one such as slide or creep or it can be a potential one, such as rock fall. This characterization does not include any forecasting of the events. Meanwhile, *hazard (H)* refers to a probability of occurrence of a danger. The period of time may be indicated in relative terms for different types of hazards. Landslide hazards may be analyzed at regional (small scales: 1:50,000-1:25,000) as well as at larger scales greater than 25,000 scale. The studies at regional and semi-regional scales are generally based on empirical approaches, whereas the detailed studies are based on analytical methods.

On the other hand, *Risk* (R) refers to the nature of damage likely to be caused if the failure occurs. The damage may be in the form of loss of life and injuries and/or loss of land and properties. Extents of damages are dependent on existing land use patterns of areas likely to be affected and the population. Hence, risk (R) is a function of hazard and the damage potential, i.e.,

$$R=f(HP, DP)$$

where *HP* - hazard probability and DP - damage potential

Risk assessment may be undertaken after evaluating the nature of hazard of a slope and its damage potential.

Table I Damage Potential (DP) for Human Dwellings. Source: (GSE, 2014)

No. of dwellings likely to be affected/damaged	Type of DP
<2	Very low DP
2-5	Low DP
5-10	Moderate DP
10-50	High DP
>50	Very high DP

Landslides can't be associated solely with one definite source; rather the factors that contribute to make slopes unstable begin with the depositional environment of rock and soil, and subsequent topographic and geological adjustments and related processes taking place in the subsurface such as erosion, weathering, groundwater flow and continuous pull of gravity. Finally, heavy rainfall, earthquake, human activities, i.e., deforestation poor land use, excavations for construction, mining trigger landslide processes. In order to carry out feasible landslide mitigation measures, knowledge of the subsurface structure and physical properties of constituting earth materials is required. Normally, only surface examinations of landslide areas provide limited information in understanding the causes extents and causes of landslides. For deep-seated landslides, it may be impossible to define its rupture surface by surface inspection alone. Instead boreholes and geophysical data are very useful to provide much needed information for a comprehensive landslide zone assessment.

Particularly, geophysical techniques are preferable because of their lower cost, extensive lateral and depth coverage with minimum or no damage to the natural environment. They provide valuable results to define the composition (physical properties), geometry (internal structures) of landslides, revealing effect of groundwater, of sliding materials, and direction of mass movement (Göktürkler et al., 2008).

1.1.2 Landslides in Ethiopia

In Ethiopia landslide problems are common in the central, northern and southwestern highlands and nearby rift margins, they result in loss of human life, property and severe damage to agricultural lands. Different researchs also show that landslides have considerable impacts on infrastructures, fertile farm lands and natural environment (Lulseged Ayalew, 1999; Kifle Woldearegay, 2005). In the years 1990-1998 alone, landslide-generated hazards have claimed about 300 human lives, damaged over 100 km asphalt road, demolished more than 200 dwelling houses and devastated in excess of 500 hectares of land in different areas of the highlands of Ethiopia (Lulseged Ayalew, 1999).

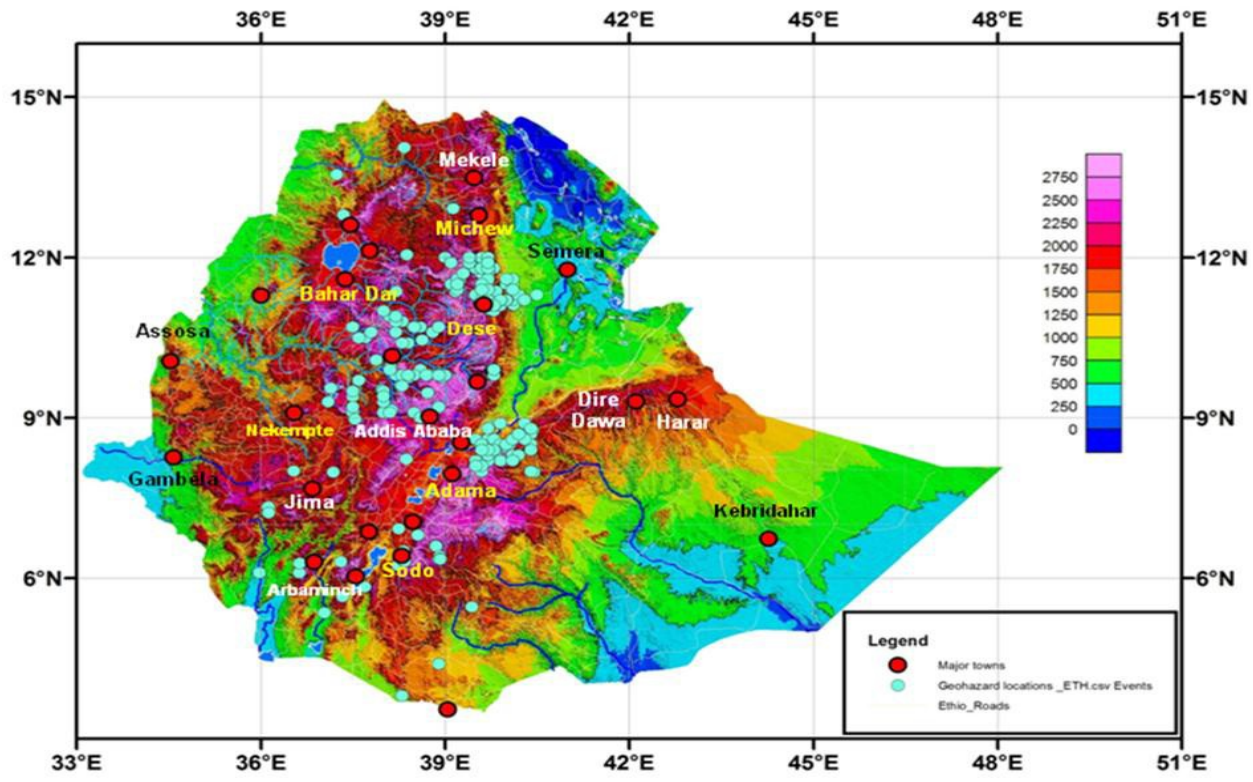

Figure 1. 1 Locations of landslide occurrences in Ethiopia (shown as blue dots). (Data source: GSE, unpublished compilation by Getnet Mewa).

As cited in Kifle Woldearegay (2005), 135 human lives have been lost, about 3500 people were displaced and an estimated 1.5 million US Dollar worth property has been damaged in the highlands of Ethiopia in the years 1998-2003. Few sites of landslide have been investigated in Ethiopia previously. In the northeastern highlands; Desssie town and southeastern highlands also experience similar cases of landslide hazard, the area around the twon of Bonga is one good example (EIGS, 1998). All of the landslide events have been observed to occur following a heavy rainfall along with a number of pre-conditioning attributes. These attributes include proximity to drainage, irrigation channel, infrastructure (road) development,which usually have the effect of undercutting the property of geologic formations and the soil condition(EIGS, 1998).

1.1.3 Landslide history and impacts

The present study area is located on the western rift escarpment and it is covered by thick colluvium materials and highly weathered volcanic rocks. During the construction of road heading from Arbaminch to Konso through Gidole town, about 50 m thick colluviums were cut for the road alignment (EIGS 2014). Together with the available shallow groundwater and steep morphology, the whole mass started to move and subsequently blocked the new aligned road before the road construction was finished. This mass movement caused active and huge landslides, which directly affected farm lands, settlement area and the road itself.

Deep seated slide along the major rift escarpment is observed. This slide is mainly observed on the colluvium materials. As these materials are loose and highly fractured, water percolates through these fractures lead to subsequent mass movement. .

The study area is affected by new and reactivated old landslides, and new ponds are formed at different places. The deep cut at the down part of the ridges, toe areas, result in the disturbance of the entire mass. At many places the new road constructed is covered by colluvial materials caused by unwise deep cut of the material along the road. As the area is underlain by shallow groundwater, the sliding was even worse.

Table II Landslide records of the area (Adopted from EIGS, 2014).

Number of Slope Deformation		LSP – 1	LSP – 2	LSP – 3	LSP – 4
Near Town, Village		Gidole	Gidole	Gidole	Gidole
Coordinate	Easting	319760	319473	319495	321115
	Northing	627125	626777	624801	623761
	Elevation	1676	1747	2037	1939
Date		27/11/2013	27/11/2013	28/11/13	28/11/2013
Slope Deformation		Single	Single	Complex	Single
Type of Slope Deformation		Slide	Slide	Falls, Slides	Slides
Rock/Soil Type		Colluvium Material	Colluvium Material	Colluvium Material	Colluvium and Fractured Rock
Hydrogeology		Dry	Dry and Undrained depressions	Dry and Undrained depressions	Dry
Degree of Activity		Active	Active	Active	Active
Cracks		Yes: Width (50 cm), Depth (1 m)	Yes: Width (50 cm), Depth (0.5 m)	Yes: Width (50 cm), Depth (1 m)	Yes: Width (20 cm), Depth (0.5 m)
Triggering Factors		Water Saturation, Change of Slope geometry and Human Activity	Water Saturation, Change of Slope geometry and Human Activity	Water Saturation, Change of Slope geometry and Human Activity	Water Saturation, Change of Slope geometry and Human Activity
Land Use		Field	School	School	Urbanized Area (Settlements)
Endangered Objects		Farm land and Road	School and Road	School	Road and Settlement

As presented in Table 2, the landslides are both single and complex. The major types of deformations observed are slides and rock falls. The landslides extend from 30 meters to more than 300 meters with slope inclination up to 40°. Colluvium material covers the slope surfaces together with highly fractured rocks. The major triggering factors are water saturation, change of slope geometry and human activity (road construction and farming). Settlements, schools and farm lands are endangered objects by the landslide occurrence in the study area (EIGS, 2014).

Below additional photos are presented which shows how much the area is affected by the improper road construction activities and the subsequent landslide and the present landform:

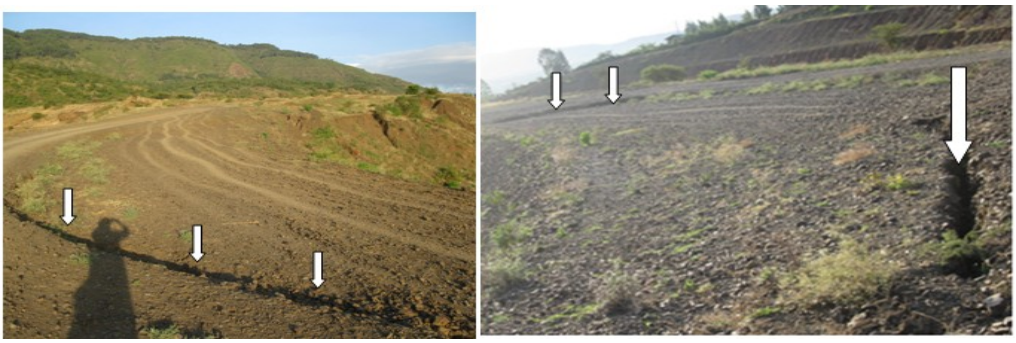

Figure 1. 2 Cracks across the road

Figure 1. 3 Collapsed Retaining Wall and the Resulted Mud Flow

Figure 1. 4 Deep Excavation in the Pyroclastic

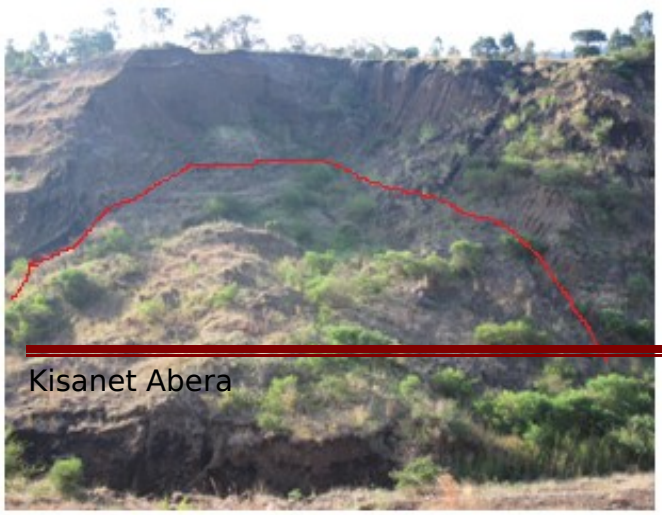

Figure 1. 5Rotational Landslide

Figure 1.6 Debris slide

Figure 1. 7 Damaged Road by Landslide

1.2 Description of the Study Area

1.2.1 Location of the study area

The landslide occurrence close to Gidole town, which is the subject of this research, is relatively an old phenomenon, but was reactivated recently. Geographically, the research area is found in Southern Nation, Nationalities and People's Regional State, Derashe Zone between Welaite Kebele and Gidole town. It is located about 540km south of the capital city Addis Ababa, 50km SW of Arbaminch town or 5km NE of Gidole town. It lies at the western margin of the Main

Ethiopian rift approximately located at 37°22'14.73" E longitude and 5°40'35.54" N latitude. The altitude within and around the site varies in the range of 1200 – 2040 mm a.m.s.l.

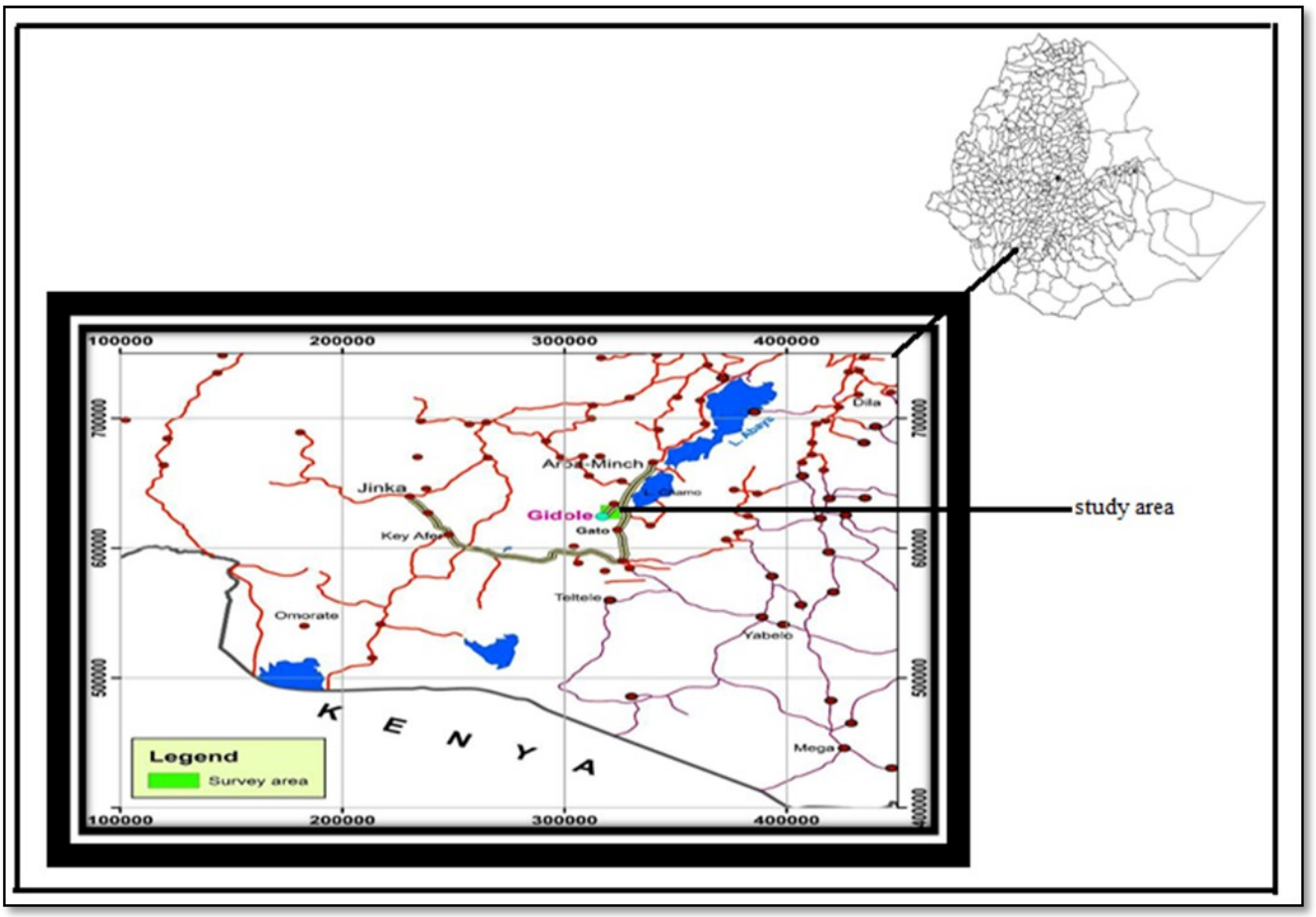

Figure 1. 8 Location map of the study area

1.2.2 Geomorphology

The study area is located at the margin of the western escarpment of the Southern Ethiopian Rift. In general, the elevation drops from more than 2400 m around Gidole town in the west to 1200 m inside the rift floor in the east (Figure1.3).

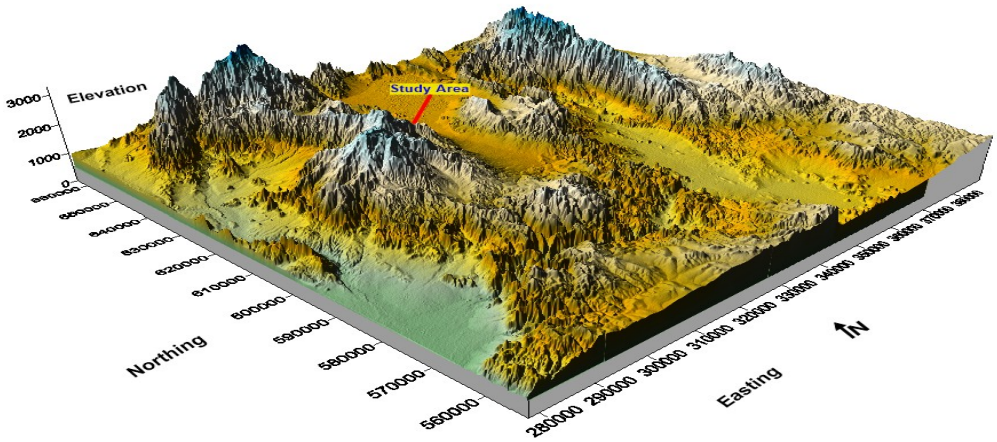

Figure 1. 9 Geomorphological map of the Study area (generated from the 90m resolution DEM data).

1.3 THE Research Problem

The landslide around Gidole has brought considerable damages on settlement, farm land, communal properties (schools, clinics,) and infrastructures. Particularly, the road heading from Arbaminch to Konso was planned to pass through Gidole town was later abandoned after due to major landslide occurred at different places. The project serves as classical example showing how poor knowledge of the subsurface geology and inadequate consideration of such features can end up with unexpected outcomes. Even though no official data are available, from oral communications with project personnel at site suggested that initially about 100 million birr was allocated by the government to construct the road but unwise deep excavations of the already unstable natural slopes have triggered serious landslide problems. To mitigate the problem the project has attempted to construct a 200m long retaining wall. Unfortunately, except escalating the project cost by more than double and causing additional load to the slopes, it couldn't help to mitigate the problem and, therefore, construction of the most severely affected segment of the road between Welaite and Gidole (about 6 km long) was abandoned. Therefore, this research was proposed to study the site conditions in-depth and using multidisciplinary geophysical techniques with an ultimate goal of generating substantial inputs contributing to the road reconstruction as well as rehabilitation works.

a) b)

Figure 1. 10 Landslide that affected the road (a), damage of the road which was under construction, but was abandoned later (b) and rock fall damaged the retaining wall.

1.4 Research Objective

1.4.1 General Objective

The principal objective of the current research is to investigate the overall characteristics of the landslide occurred between Welaite kebele and Gidole town, just on the newly constructed Arbaminch-Gidole-Konso road, and understand the triggering factors and sliding mechanisms.

1.4.2 Specific Objective

To attain the above stated general objective the following specific objectives shall be addressed:

- ✓ Study the physical characteristics of the underlying rocks and assess their suitability for foundation of civil engineering structures (roads, bridges, buildings) to be constructed in the area.
- ✓ Determine extents of the landslide affected zones and outline geometry of the main slip plane (failure surface) over which mass movement is taking place.
- ✓ Delineate structural weak zones in the subsurface that are critical locations for surface ruptures leading to loss of life and infrastructure damages.
- ✓ Clarify the main possible factors that trigger/ aggravate the landslide processes and propose landslide hazard mitigation measures;

1.5. Methodologies

To achieve the above-stated objective of the research, three stages shall be employed:

Stage I: collection and analyses of secondary data

This stage includes collection of secondary data from literatures (textbooks, journals, various official documents, published and unpublished papers) from various professionals on geophysical investigations carried out for landslide investigations conducted by the Geological Survey of Ethiopia (GSE), Ethiopian Roads Authority (ERA), Addis Ababa University (AAU) and few others.

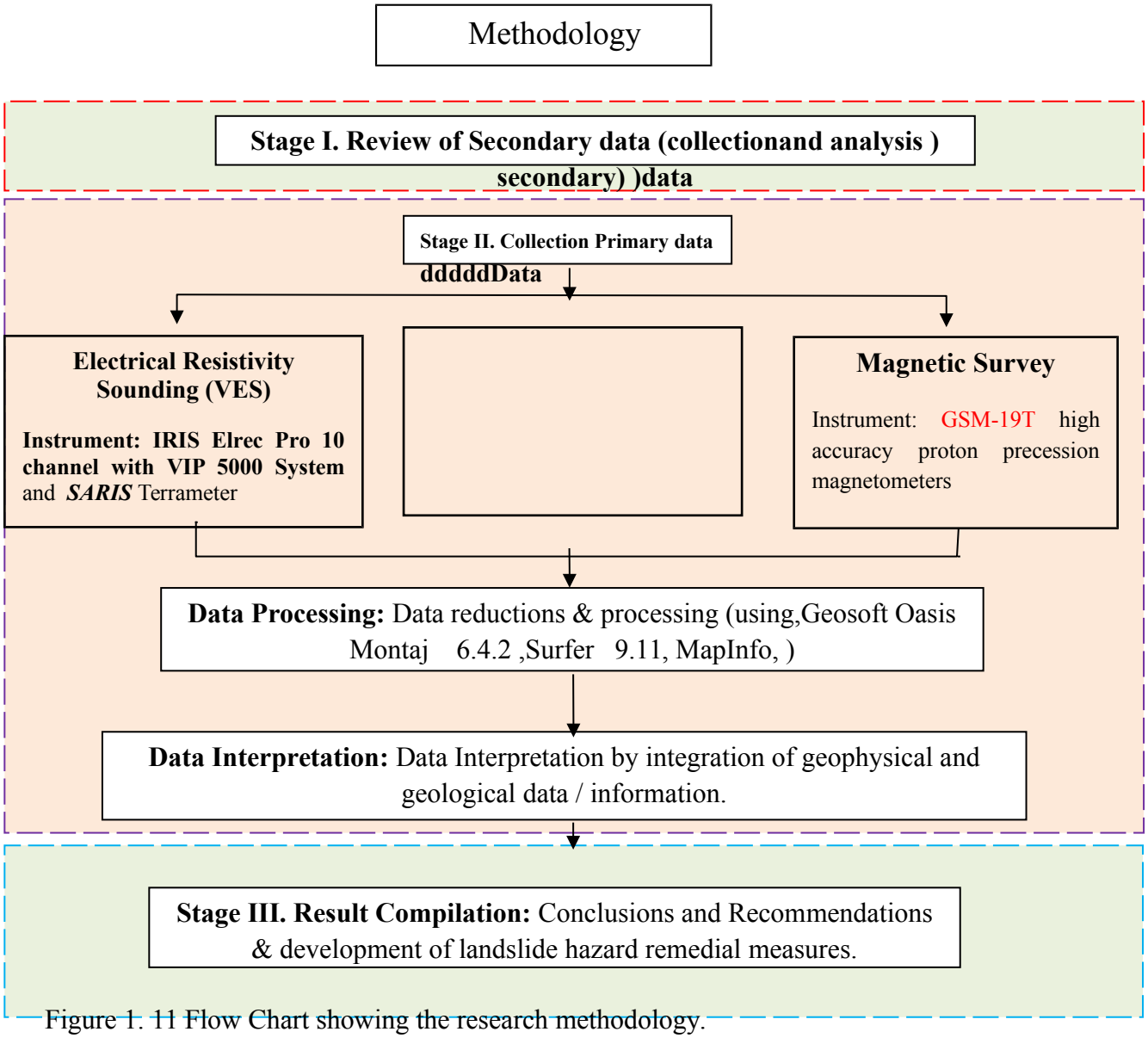

Figure 1. 11 Flow Chart showing the research methodology.

Stage II: Collection of Primary data pertaining to the present study. The methods employed at the site included Electrical Resistivity Sounding (VES) and Magnetic Survey. Geophysical data were collected along selected traverses crossing the landslide zone and randomly along foot paths. .
The Geosoft Oasis Montaj (v. 6.4.2) geophysical data processing and analyses tool as well as ArcGIS 10.1, Surfer 9.11, WinResist and RESIX-IP software are employed. .

Accordingly, maps and models are produced and interpreted to obtain information set out in the project objectives. The generalized flow chart of the methodological approach deployed for this investigation is described in Figure1.11.

1.6 Review of previous work

The following are some of the works in different landslide susceptible areas of Ethiopia:

Engineering geophysical investigation along a proposed alternative route of Blue Nile Gorge has been conducted (EIGS, 1994). The survey methods used were refraction seismic, electrical resistivity (VES and profiling) and magnetic with the objectives of determining depth to the bed rock, locating possible structural features, and studying the nature of the overburden material.

Investigations of landslide problem using geophysical techniques around Debresina–Armania main road have been conducted (Gebreselassie Gebreanenia, 2013). Based on this work, Electrical Resistivity Tomography (ERT) and Magnetic Survey were carried out with the objective of identifying the triggering mechanisms of the landslide problem and recommend possible mitigation measures.

The integrated engineering geological and geophysical investigations for landslide studies in Bonga town and its surroundings have been conducted (EIGS, 1999). The geophysical methods, which consisted of Refraction seismic, Vertical Electrical Sounding, Electrical resistivity profiling and magnetics, were conducted along 27 profiles covering a total length of 7.6 km.

Some researchers have visited the study area and its surrounding for different purposes but there was no works conducted geophysical investigation for the landslide problem mitigation on the study area.

EIGS (2014) conducted different geological and engineering geological investigations for land slide studies in with the objectives of study in detail the landslide hazard, which was caused by the construction of new road towards the Gidole town.

1.7 Limitation of the Study

All efforts are being made to carry out the study in a systematic manner, well supported with actual field data. However, these efforts were made under limitation of field vehicles, accessibility problem due to heavy rainfall that, absence of relevant secondary data providing better picture about status of the problem as well as shortage of time and financial support.

1.8 Thesis Layout

This thesis is organized in to six chapters. The first chapter is the introduction part which includes the general description of the study area, discusses statement of the problem, objectives, and research methodology. The second chapter is devoted to the analysis / assessment mostly with the work of previous researchers that includes geology, hydrogeology, climate, tectonic and seismicity of the study area and its surroundings. Chapter three covers the theoretical background for the geophysical methods employed in this study. Chapter four describes the complete survey procedure, data acquisition, data processing, and presentation of the different methods of the results. Chapter five incorporates integrated results and interpretations of geophysical methods. The last chapter contains conclusions and recommendations of the overall work of the thesis.

CHAPTER-2

2. GEOLOGY, HYDRO GEOLOGY AND TECTONICS OF THE STUDY AREA

2.1 Regional Geology

The geology of southern rift valley and its escarpment is conveniently divided into different major groups of rock units, based on age, being Precambrian to early Paleozoic crystalline basement, tertiary volcanic-sedimentary rocks overlain by felsic lavas and pyroclastics, quaternary alluvial and lacustrine deposits and recent volcanic cover.

2.1.1 Precambrian crystalline basement rocks

The Precambrian basement rocks of the region have a wide range of compositions, varying from ultramafics to quartzofeldspathic gneiss. Migmatization, pegmatization and granitization of these rocks are highly variable.

Mafic hornblende gneiss referred as Konso gneiss (Kazmin, 1972), amphibolites and mafic granulite underlie a large area from Segen River up to the southern side of Gidole highland. They are relatively dark gneisses, usually rich in hornblende and poor or lacking quartz.

The quartzo-feldspathic gneiss underlies large tracts of ground between Jinka and the north end of the Hamar range. In the area of Jinka and Beto, pink and light grey quartzofeldspathic are foliated, biotite-bring commonly migmatitic and pegmatitic rich in K-feldspar. Plutons of gabbroic and ultramafic rocks also occur within the mafic gneisses and granulites to the west-northwest of Konso.

2.1.2Tertiary volcanic-sedimentary rocks

A. Sedimentary rocks of Pre-rift basal red sandstone

The unconformity at the base of the tertiary volcanic succession throughout a large part of the region is marked by a thin unit of red sandstone and conglomerate 4 to 40 m thick. Outcrops are usually too small to be shown on small scaled geological maps. Davidson (1983) suggested the red sandstone represented an erosional surface in southwestern Ethiopia and favored an early

Tertiary age for it. Fossils were not observed in any of the occurrences, but the ages of the basalt flows which directly rest on the red sandstone limit its minimum age.

B. Pre-rift volcanic succession

The pre-rift succession of Tertiary volcanic rocks is subdivided on lithologic grounds into basaltic, intermediate and salic units. Rocks of the basaltic unit are referred to as the 'early flood basalts or lower basalts'.

A two-stage succession underlies the Gidole highland. Up to 600m of sub-horizontal basalt flows lie between the basal sandstone and overlying salic flows on the east and south flanks of Mount Guroza whose salic cap, tilted very gently to the east-southeast, is a minimum of 300m thick.

The lower basalts are the most widespread volcanic unit in the rift margin of Omo valley including the study area. The Lower Basalt is characterized by thick, extensive lava flows that locally show columnar jointing and weathering. Numerous small intrusions of rhyolite, trachyte and a cluster of phonolite occurs North West of Mount Guroza. The large intrusions are centered in thick accumulations of salic flows, mainly blocky rhyolites or trachytes with associated coarse fragmental rocks (Moore and Davidson, 1978).

C. Post-rift succession

Recent volcanic units

The Lake Chamo basin is characterized by the occurrence of recent volcanic units: the Nechsar Basalt, Segen basalt cones and Chamo cinder cones were emplaced during the middle to late Pleistocene (Ebinger et ale 1993).

2.1.3 Quaternary alluvial and lacustrine deposits

Eroded materials have been deposited in Chamo Lake and lower part of the Omo basin as a thick sequence of Quaternary alluvial deposit. 20 m of lacustrine sediments of Plio-Pleistocene age is also deposited in the valley western to Gidole highland. The sediment deposit is composed of buff, brown and grey sands, silts and clays.

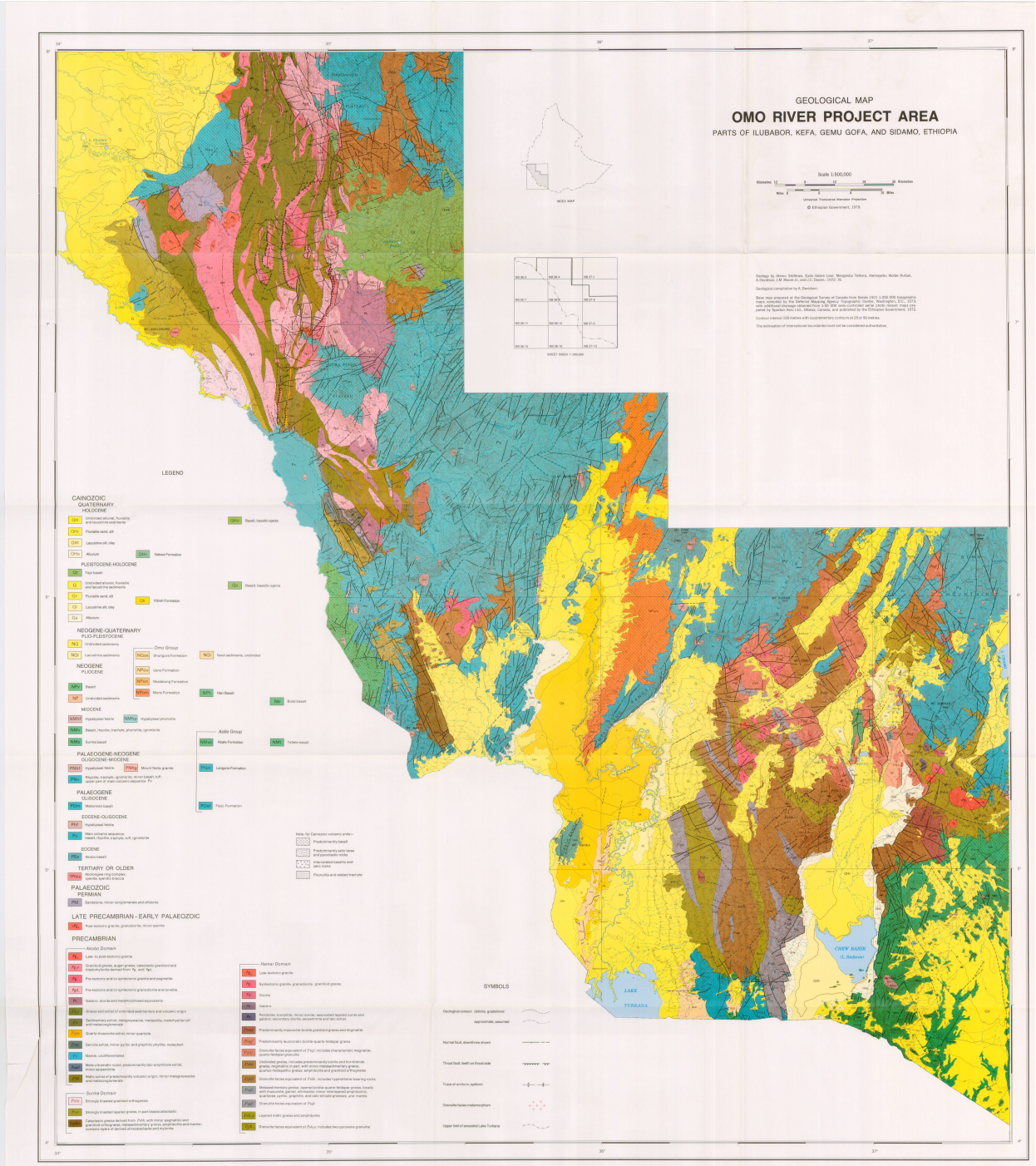

Figure 2. 1 Geological Map of Omo Basin (Scale 1: 500,000) (adopted: Davidson, 1983)

2.2 Local Geology of the Study Area

2.2.1 Porphyritic Basalt

This is the most widespread volcanic unit in the study Area. The Basalt is characterized by thick, extensive lava flows that locally show weathering. The exposure on the foot of the ridge is light grey, slightly vesicular, columnar jointed and more or less horizontally layered. The basalt outcrop exposed at the junction of the existing and abandoned roads is also light grey, but highly weathered porphyritic olivine feldspar basalt which lies directly on top of the red sandstone Figure2.2.

Figure 2.2 Highly weathered Porphyritic basalt

2.2.2 Pyroclastic flow deposit

This 5m thick deposit is exposed on the foothill of Gidole horst overlaying the weathered basalt unit. Top of the layer is yellow, well sorted and no coarse materials are observed in the stratification. The bottom layer however is characterized by poorly sorting, poor or no bedding, discontinuous trains of large fragments and alternating coarse- to fine-grained layers. The pyroclastic flow

deposits are commonly strongly oriented parallel to depositional surfaces towards east direction (see Figure2.3).

.

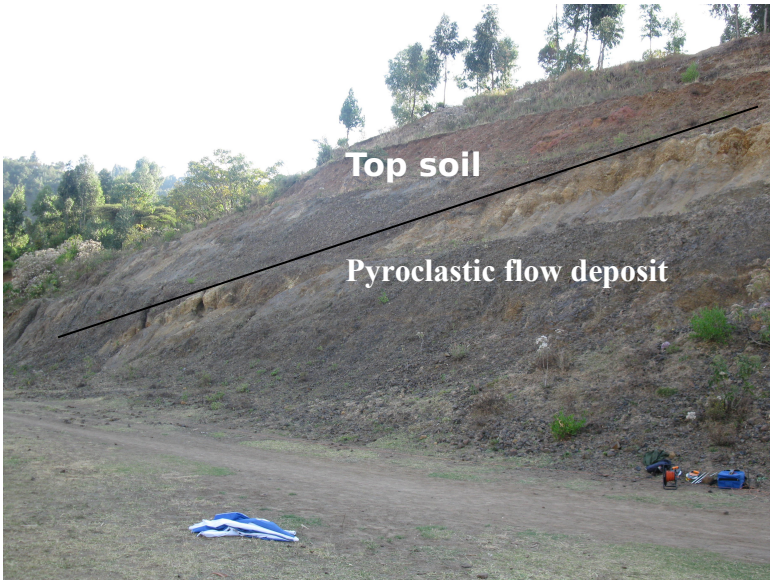

Figure2.3 Pyroclastic deposit exposed at the upper junction of the road

2.2.3. Felsic rocks

Thick accumulation of salic flows, mainly blocky rhyolites or trachytes with associated coarse fragmental rocks is exposed in the peak of Gidole highland including Gidole Town.

2.2.4 Colluvial deposits

These unconsolidated sediments that have been deposited at the base of the Gidole horst by slow continuous down slope landslide. The upper layer of this exposure up to 30 m thick is marked by pockets of poorly consolidated gravel with sands and tuffaceous silts and clays Figure2.4. The conglomeratic deposit at the bottom layer is 5m thick, light grey and poorly sorted. It is a clastic supported cobble conglomerate, cobbles of rocks from the uphill volcanic material.

Figure2.4 Thick colluvial deposit collapsed along the road side

-

2.2.5 Red Basal Sandstone

Red basal sandstone is outcropped at two localities on the excavated slope of the abandoned road. As the outcrops are too small to be shown on the accompanying geological map, their distribution is mapped with bold line in the local geological map Figure2.7.

The red sandstone outcropped at the eastern tip of the abandoned road is 2 to 3 m thick, medium to coarse grained, thickly bedded and dips about 25° W (Figure2.5). It is reddish, friable and texturally matured. The bottom part of the bedding is highly weathered, reddish to brown and consists of thin layers of sand and sandy silt.

Figure2.5 Inclined strata of red basal sandstone in the study area

The red basal that blankets the steep side of the excavated road near Wolayte spring is about 10 m thick, relatively resistant to erosion and formed continuous ledge and blanket beneath the basaltic flows that characterized Gidole highland as shown in Figure2.6.

The upper part consists of well sorted sandstone, massive, red to brown colored while the lower part is weathered, poorly sorted medium to coarse grains with scattered angular to subangular pebbles and cobbles.

Figure2.6 Red basal blankets steep side of the road

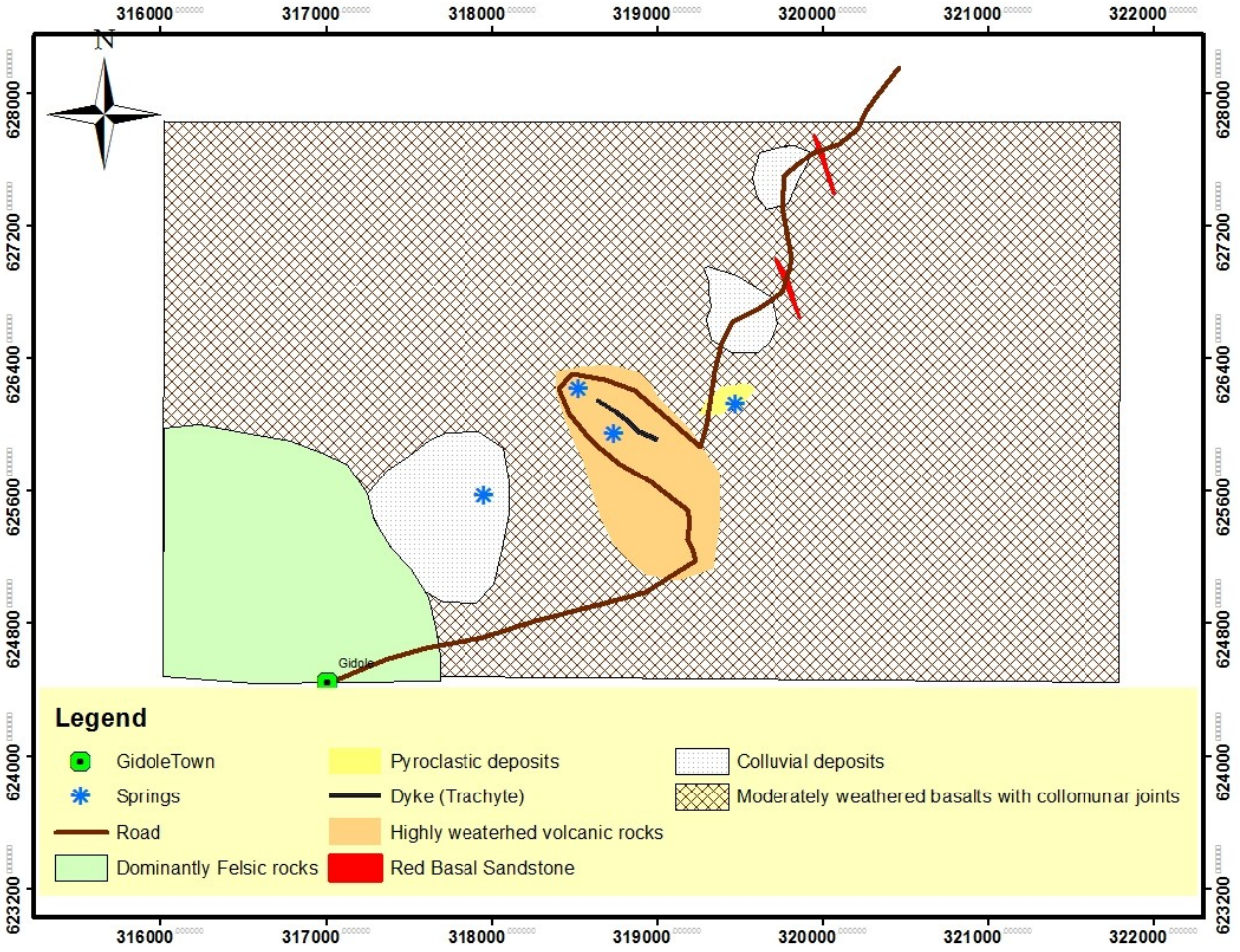

Figure2.7 Local Geology of the Area (Scale 1: 50,000)

2.3 Geological Structures

Faults

NNE-SSW, NNW-NNE and NE-SW trending faults are common in the eastern part of Gidole highland (Figure2.8). They are normal faults up to several kilometers long and form the major boundaries of the Gidole ridge and the rift basin.

The longest and best defined of these faults traversed by the main highway to Gidole Town is the regional fault which separates Gidole horst from the Rift valley floor. It extends NNW to SSE where it is displaced by a NE trending fault at 5km northwest of the road (Figure2.8).

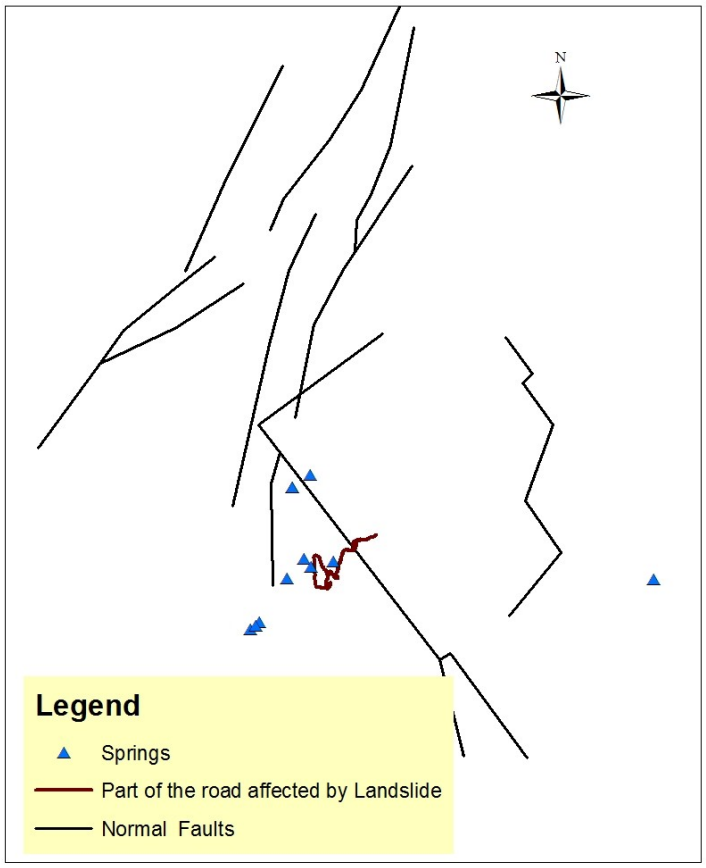

Figure2.8 Springs associated with the Geological Structure(Scale 1: 50,000)

Joint

The most commonly joint types observed in the study area are columnar joints. It is highly fractured and weathered along with it is also grayish. At some places this unit is intercalated with felsic rocks (Figure2.9). The Columnar joints which were 0.05 – 0.2 meter aperture. They can be one factor for the sliding problem of the study area.

Figure2.9 Columnar joints

2.4 Hydrogeology and Ground water flow system of the Study area

Much of the water-bearing zones in the Gidole highland and the rift escarpment are within the weathered and fractured basalt and locally in inter-bedded river gravels and unconsolidated sedimentary deposits.

Many fault- controlled springs are aligned along NNW-SSE and NNE-SSW direction indicating the importance of these major rift fault systems in controlling the movement and occurrence of groundwater. Groundwater migrates to the east following these faults as well as contact zone between the weathered basalt and massive trachyte dyke on the western tip of the collapsed road.

The large hydraulic gradient and the presence of faults have resulted in the formation of different discharge areas at different elevations, mainly along the escarpment of Gidole horst and at the feet of highland volcanic terrain. The large elevation difference between the rift floor and the top of the ridge favor the formation of local, intermediate and regional flow systems. Different springs and seepage zones represent these flow systems.

Figure2.10 Natural pond formed by springs at the abandoned road

2.5 Tectonics and Volcanism

The area has undergone several tectonic events and consists of four tectonic units: the plateau, south-western margin of the plateau, escarpments and rift areas. The area is wholly controlled by rift tectonics and is a part of the East African Rift System (EARS).

Volcanism in Southern Ethiopia began in the middle to late Eocene. The history of the uplift in the study area thus most probably began shortly after the inception of volcanism of the main – basal succession. The initiation of the horst and graben system had reached something very like its present form by early Pliocene time. The major uplift and graben faulting in the southern part of the MER occurred in the early Pleistocene according to Ceri (1972). Forming of the proto – Ethiopian rift about 25 million years ago and starting from the late Oligocene, the main evolutionary events of the rift system is supposed by Zanettin (1978).

CHAPTER- 3

3. FUNDAMENTALS OF THE GEOPHYSICAL METHODS OF INVESTIGATION

3.1 Preamble

Geophysical investigations of interior of the Earth's interior involve taking measurements at or near the its surface that are influenced by the internal distribution of physical properties. Geophysical investigations have many advantages such as, they are flexible, relatively quick, non- invasive and provide information about the internal structure of soil or rock masses, and allow investigation of a large volume and/or area.

Geophysical methods are applied in various types of landslides with slope angles varying from few degrees (earth slide) to high angles or vertical (rock fall). The depth penetration also varies in a wide range few meters to over kilometers and the targets can be broadly classified in to two: By far, the major target is to delineate the location, vertical and lateral extents of the sliding masses or, equivalently, failure surfaces. An additional and implicit target is mapping of internal structures of landslide zones.

Four main different possibilities can be expected: Case I: geophysical contrasts are due to the lithological changes (layering, tectonic contact or pre-slide weathering) and the failure surface mainly coincides with a geological interface or layer. Case II: geophysical contrasts are also controlled by lithological variations but the failure surface cuts the structure in a more complex way and may be or not deduced from the geophysical image, depending on the landslide velocity, heterogeneity of the materials and resolution of the technique used. Case III: the failure surface (or potential failure) is directly detected, mainly by propagation methods. Case IV: the landslide develops in a globally homogeneous layer and alters its characteristics. The geophysical contrast then arises between the slide and the unaffected mass from the cumulative or separate action of the mechanical dislocation, the weathering and an increase of water content.

The second target of geophysical prospecting is the detection of water within the slip mass, for which electrical methods are often applied effectively. Thus, geophysical methods are implemented with considerations of the above mentioned possible scenarios (Bichler *et al.*, 2004).

3.2 The Electrical Resistivity Method

The purpose of electrical resistivity survey is to determine the subsurface resistivity distribution by making measurements on the ground surface. Any electrical resistivity survey depends on a mineral compositions of minerals constituting the rocks and soil masses, grain sizes, contents of water (degree of saturation) and degree of mineralization, temperature, pressure, etc (Robert and William, 1981).

3.2.1 Principles of Resistivity Method

The well-known resistance R, in ohm, of a wire is directly proportional to its length L, and is inversely proportional to its cross-sectional area A. That is:

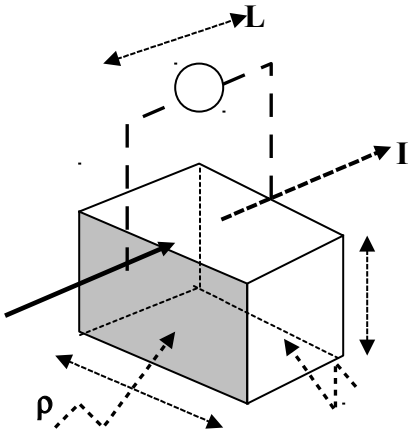

$$R = \rho \frac{L}{A} \qquad (3.1)$$

where ρ is the constant of proportionality known as the electrical resistivity and it describes the characteristic of the materials, which is independent of its shape or size.

According to Ohm's law, the resistance is given by

$$\mathbf{R} = \frac{\Delta V}{I} \qquad (3.2)$$

where ΔV is the potential difference across the resistance and I is the electric current flowing through the material.

The resistivity ρ of homogeneous and isotropic materials in the form of regular geometric shapes, such as cylinder, cubes are determined from the following equation;

$$\rho = \frac{\Delta V}{I}\left(\frac{L}{A}\right) \qquad (3.3)$$

In resistivity surveys, commutated direct current is introduced into the ground via two electrodes. The potential difference is then measured with another pair of electrodes. The current and potential difference measurements together with the parameter that determines the distribution of the electrodes over the ground are used to calculate resistivity of the ground.

The electric potential V caused by a point source emitting electric current I into a homogeneous and isotropic medium of resistivity 'ρ' is given by;

$$V = \frac{\rho I}{2\Pi r}\left(\frac{1}{r}\right) \qquad (3.4)$$

where, $r^2 = x^2 + y^2 + z^2$ is the distance between the point of measurement and the current electrode.

For a semi-infinite medium, which is the simplest earth model, and with both current and potential point electrodes placed at the Earth surface (z = 0), equation (3.4) reduces to;

$$V = \frac{\rho I}{2\Pi}\left(\frac{1}{r}\right) = \frac{\rho I}{2\Pi}\left(\frac{1}{AM}\right) \qquad (3.5)$$

where, AM is the distance on the Earth's surface between the positive current electrodes (A) and the potential electrode (M). When two current electrodes (A and B) are used and the potential difference (**ΔV**) is measured between two measuring electrodes, 'M' and 'N', we obtain;

$V_{AM} = \frac{\rho I}{2\Pi AM}$, is potential at 'M' due to positive electrode 'A'

$V_{AN} = \frac{\rho I}{2\Pi AN}$, is potential at 'N' due to positive electrode 'A'

$V_{BM} = \frac{\rho I}{2\Pi BM}$, is potential at 'M' due to negative electrode 'B'

$V_{BN} = \frac{\rho I}{2\Pi BN}$, is potential at 'N' due to negative electrode 'B'

The total net potential at 'M' is then,

$$V_M = \frac{\rho I}{2\Pi}\left[\frac{1}{\frac{1}{AM} - \frac{1}{BM}}\right]$$

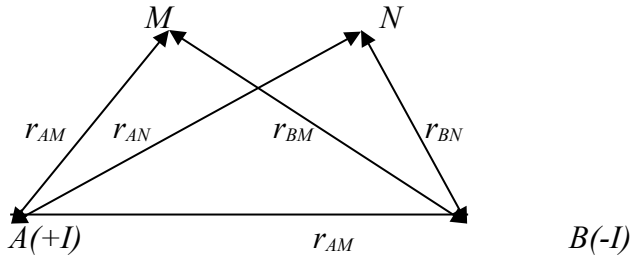

The total net potential at N is then;

$$V_M = \frac{\rho I}{2\Pi}\left[\frac{1}{\frac{1}{AN} - \frac{1}{BN}}\right]$$

Therefore, the net potential difference is;

$$\Delta V = \frac{\rho I}{2\Pi}\left[\frac{1}{\frac{1}{AM}-\frac{1}{BM}-\frac{1}{AN}+\frac{1}{BN}}\right] \qquad (3.6)$$

Rearranging equation (3.6), we can express the resistivity ρ by;

$$\rho = \frac{2\Pi}{\frac{1}{AM}-\frac{1}{BM}-\frac{1}{AN}+\frac{1}{BN}}\left(\frac{\Delta V}{I}\right) \qquad (3.7)$$

Equation (3.7) is a fundamental equation in direct current electric prospecting.

The factor $\frac{2\Pi}{\frac{1}{AM}-\frac{1}{BM}-\frac{1}{AN}+\frac{1}{BN}}$ is known as the geometric factor of the electrode arrangement and generally is denoted by 'K'.

Then, equation (3.7) can be rewritten as;

$$\rho = K\left(\frac{\Delta V}{I}\right) \qquad (3.8)$$

If the measurement of resistivity (ρ) is made over a semi-infinite space of homogeneous and isotropic material, then the value of resistivity computed from equation (3.8) will be the true resistivity of that material. However, if the medium is in heterogeneous and anisotropic then the resistivity computed from equation (3.8) is called an apparent resistivity (ρ_a).

The value of the apparent resistivity is a function of a number of parameters: the electrode spacing, geometry of the electrode array, and the true resistivity and other characteristics of the subsurface materials, such as layer thicknesses, angles of dip, and anisotropic properties. From these we can infer that the apparent resistivity, depending on the electrode configuration and on the geology, may be a resistivity (Zohdy, 1980).

3.2.3 Types of Resistivity Surveys

Electrical resistivity techniques have been used in many geological formations for characterizing the subsurface. There are two basic types of resistivity investigations: profiling and sounding (i.e., lateral and depth investigations respectively). A combination of both has also been possible through the development in electronic switching that has resulted in improved data acquisition

and interpretation. Moreover, the earlier techniques although still widely used were considered very labor intensive and the development of the multi-electrode surveys has been able to reduce this aspect of the survey (Heather et al., 1999).

3.2.3.1 Electrical Resistivity Sounding

The procedure involved in vertical electrical sounding is primarily based on the assumption that the subsurface has a horizontal stratigraphy. In other words, it consists of discrete, horizontal, homogeneous and isotropic layers. Electrical resistivity sounding (also referred to as electrical drilling) is a process by which depth investigations are made through successive resistivity measurements done with regularly increasing electrode separations keeping the array center and its orientation fixed (Figure.3.1). As the distance between current probes is increased, there is also an increased in the depth at which the current penetrates below the surface of the distribution below the center of the array is determine (Loke, 2001).

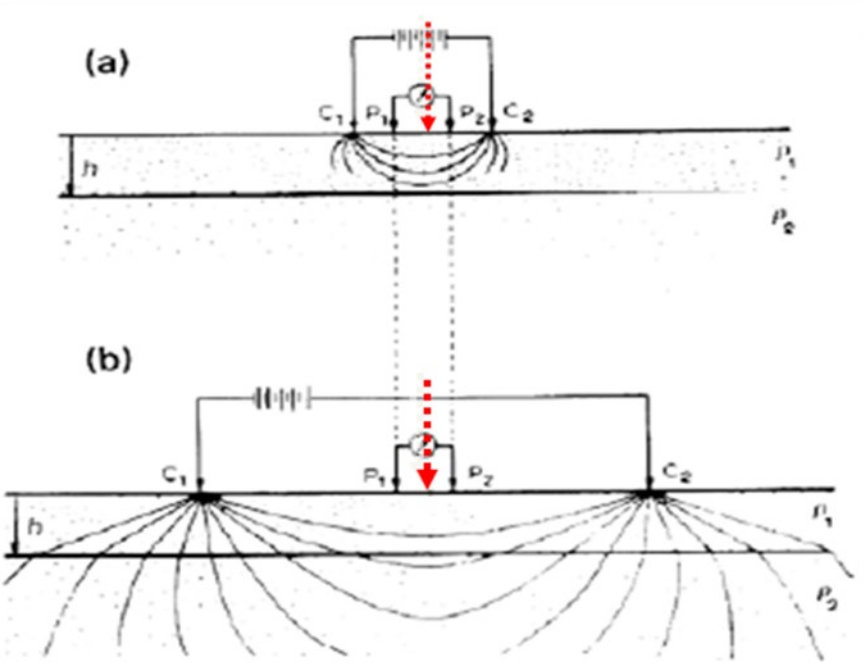

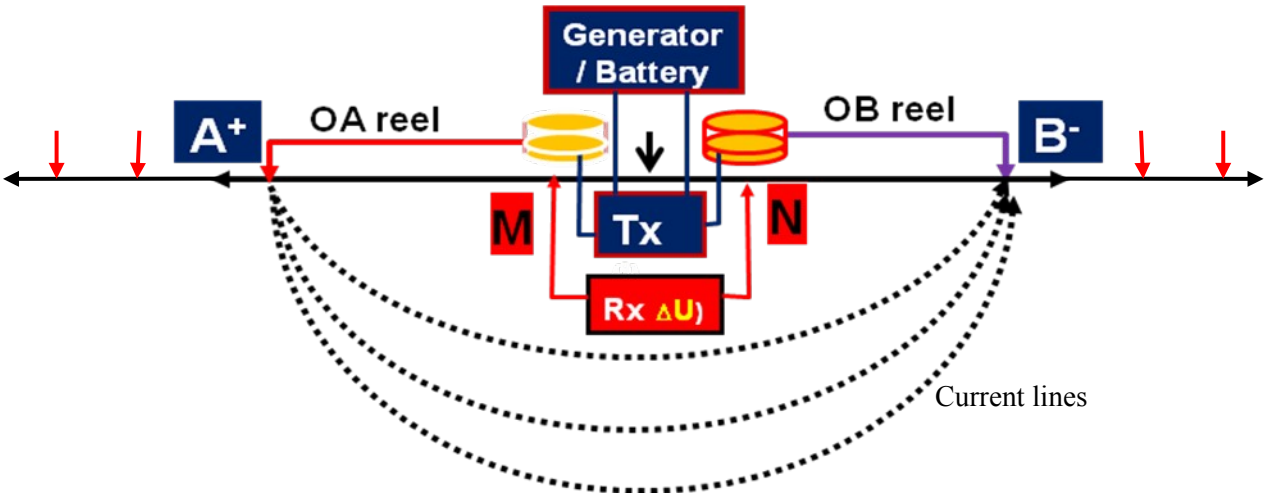

Figure3.1 Schematic electrodes lay out for the electrical resistivity sounding.

The Fundamental problem of electrical resistivity sounding is finding the solution to the problem of potential (U) field distribution due to DC sources over horizontally layered heterogeneous media.

3.1.4 Electrode arrangements in electrical profiling

There are various electrode arrangements have been designed in electrical measurements and several are occasionally employed in specialized surveys, only two-three of them are in common use (Habberjam, 1979). The most widely used electrode configurations in DC resistivity surveys are briefly discussed below

3.1.4.1 Wenner Array

This array is a symmetrical arrangement in which the points A, M, N and B are taken on a straight line such that the points are symmetrically placed at a fixed separation 'a'.

Figure 3.2 Arrangement of electrodes for the Wenner array.

The general formula to calculate is: $K = \frac{2\pi}{\frac{1}{r_{AM}} - \frac{1}{r_{BM}} - \frac{1}{r_{AN}} + \frac{1}{r_{BN}}}$, but here $AM=MN=NB=a$

Because of this the final formula for ***k*** will be reduces to: **k=2πa**

Accordingly, the apparent resistivity is calculated using the formula:

$$\rho_a = 2\pi a \frac{\Delta U}{I}$$

3.1.4.2 Schlumberger Array

Schlumberger array is a symmetric four electrodes array to which the spacing between the current electrodes is about five times greater than that of the potentials *(i.e., AB≥5MN)*. Normally, the potential electrodes (M & N) are placed at the center of current electrodes (A & B), i.e., symmetric with respect to the center of the array O (Figure3.3).

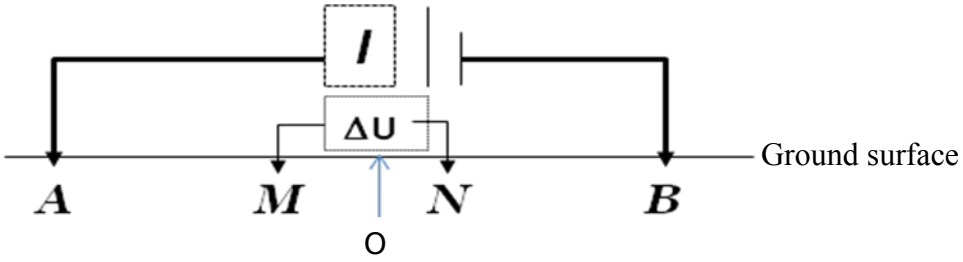

Figure3.3 Electrode arrangement of the Schlumberger Array

$$\rho_a = \frac{\Delta U}{I} \frac{\pi r_{AM} r_{AN}}{r_{MN}}$$

3.1.4.3 Dipole-Dipole Array

In this case the lengths of the current and potential dipoles are very short compared to the distance between the centers of the dipoles. In practice there are different varieties of electrode arrangements, referred as axial ($\varphi=0$ & $\beta=0$); azimuthal ($\beta=90^0$); parallel ($\beta=\varphi$); radial ($\beta=0$); and equatorial ($\varphi=90^0$).

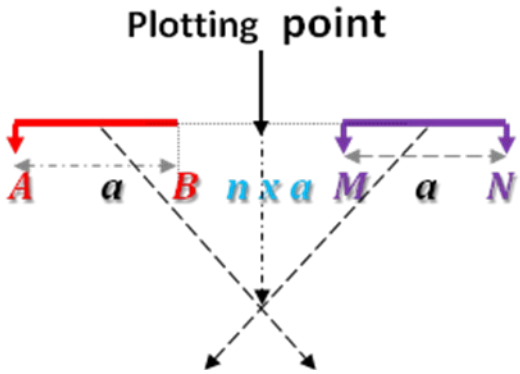

here AB is the current and MN - the potential dipoles which are equal in length (=***a***) and *n* shows the dipoles separation, or it is called dipole number.

The plotting points at any arbitrary stations are determined by drawing straight lines at 45^0 from the centers of dipoles towards each other and project the location where the two lines meet on the horizontal plane.

The array coefficient for the commonly used configuration, i.e., axial dipole-dipole array will be calculated using the formula:

$$K = \pi n (n+1) (n+2) a.$$

3.2.4 Electrical resistivity and affecting factors

Resistivity surveys give a picture of the subsurface resistivity distribution. To convert the resistivity signature in to a geological picture, some knowledge of typical resistivity values for different types of are generally characterized by high resistivity values, however, the values are greatly dependent on different features. the degrees of weathering, fracturing, and the types/properties of materials (fluids/gases) filling the fractures pore spaces. Meanwhile, sedimentary rocks have lower resistivity value due to that they are usually porous and contain higher amount of moisture / water.

- The electrical resistivity of the mineral grains constituting the rocks' skeleton

  According to their behavior of electric conductivity minerals are classified as: i) *conductors:* example Au, Pt, Ag…. These minerals are characterized by low resistivity, ≈ $\rho=10^{-6}$-10^{-4} Ω-m; ii) *semiconductors* (example: most sulfides and few oxides); iii) *dielectrics:* insulators like quartz, gypsum, anhydrite, plagioclase, mica; their resistivities vary in the range of $\rho=10^{9}$-10^{16} Ω-m;

- The electrical property of solutions filling pore spaces and fractures. Often pore spaces are filled by solution, which are represented by saline solutions. With the increasing of saline concentration C, resistivity ρ of rocks decreases.

  Pores may occur in three forms:

  - Pores of inter-granular nature, i.e., spaces left between the mineral grains as the rocks cooled and over after the rock grains were compacted. This is mostly common in consolidated sedimentary rocks, volcanic ash beds.
  - Pores in form of joints – spaces in jointed rocks. This occurs mainly in igneous rocks
  - Vugular porosity or cavities formed by solutions as in limestone or large gas bubbles as in some volcanic rocks.

  Generally, resistivity of water-bearing rocks decreases with increasing water contained in pores. In order that the rocks can conduct electricity, pores must be interconnected and filled with water. But in all three types of porosities, pores volume may consist of two parts: large voids (storage pores) and connecting pores (the finer ones).

  Experimentally, it is established that resistivity varies approximately as the inverse square of the porosity when the rocks are fully saturated with water. This relation between *resistivity* and *porosity* is explained by *Archie's law* as:

  $$\rho = a\rho_w p^{-m} \quad \text{or} \quad \rho = \rho_w Pn$$

  Here ρ - is the bulk resistivity of rock, ρ_w - resistivity of the water contained in pore structure, p – is a parameter of porosity (it mainly depends upon the porosity and structure of pore spaces). Porosity is expressed as a fraction per unit volume of rock; a is a parameter whose values is assigned arbitrary to make the equation fit a particular group of measurements and its value is slightly above or below 1 *(a=0.4-1.4); m* is a parameter characterizing whether the rocks are cemented and well-sorted granular or poorly-sorted and poorly cemented and its value is slightly above or below 2 (*m=1.3 - 2.2*).

- Degree of fracturing: resistivity depends on the degree of fracturing of rocks, amount and type of solutions filling pore spaces. Generally, fractured rocks have lower resistivities than their undisturbed equivalents.

- *Moisture content* - the fact that resistivity of rocks lying above the water table is higher than those below it is an indicative the relation existing between the between resistivity and moisture content and/or degree of saturation of the rocks. Thus, with the increasing of moisture content electrical resistivity decreases and vice versa.
- *Structures and textures of rocks:*
- Forms, sizes and arrangements of pores as well as minerals grains in rocks play great role in determining the flow of electric current. Special patterns in the arrangement of mineral grains/pores within the rock mass could be the cause for the formation anisotropic characteristics (λ) in most sedimentary and metamorphic rocks. For most rock types λ varies in the range of 1-1.5, but for stratified formations it value increases up to *3-5*.

- *Degree of chemical and physical weathering and its depth continuation:* The intensity of resistivity can also be highly affected by weathering activities. Highly weathered and fractured rocks below the water table may have resitivity about 10 times lower than their compacted and fresh equivalents.
- *Temperature and pressure: With the increasing of te*mperature resistivity of rocks composed of minerals with ionic conductivity is decreasing due to the increasing mobility of ions. However, resistivity of ores minerals with electronic conductivity increases with increasing of temperature due to increasing of random motions of electrons. But generally the electrical resistivity of the earth decreases with the increasing of temperature; at a depth of few hundred of kilometers it is about 1-0.1 Ω-m, whereas at few thousands kilometers it is almost thousands times less.
- The electrical resistivity and temperature are related in the following way:

    - $\rho_t=\rho_{18t}/[1+d_t(t-18^0C)]$

- *Character and intensity of electrochemical reactions:* That is to say oxidation and reduction reaction processes taking place at the surface of the solid mineral grains and electrolyte solutions filling pore spaces of the rock mass.

Table IIIResistivity of some common rocks is given in **(**Loke, 1999).

Rock types	Resistivity (Ωm)
Metamorphic/Igneous rocks	
Granite	5×10^3 - 10^6
Grano-diorite	1×10^6-8×10^7
Slate	6×10^2 – 4×10^7
Pyroxenites	8-10×10^3
Gneisses	8-10×10^3
Amphibolites	1×10^6-1×10^7
Marble	1×10^6 – 1 x 107
Quartzite	1×10^6 - 1 x 10^8
Basalt	5×10^3 – 1×10^5
Andesite	5×10^3 – 1×10^5
Sedimentary Rocks	
Sandstone: • Saturated with fresh water • Saturated with saline water	1×10^5 – 1×10^6 3×10^1 – 2×10^2 1 - 10
Clay: • Saturated with fresh water • Saturated with saline water	1×10^3 –1x105 1x10 – 1×10^2 1-10
Gypsum	1×10^5 – 1×10^7
Shale	20 -2 x 10^3
Limestone	50 - 4 x 10^2

3.2.3 Interpretation of VES Data

Types of curves electrical sounding over horizontally stratified media

Generally, forms of VES curves obtained over horizontally stratified media are function of layers' resistvities, thickness as well as types of electrode configurations.

A. Homogenous and isotopic medium:

If the ground is composed of a single homogeneous isotropic layer of infinite thickness (but with finite resistivity) then, irrespective of the electrode array used, the apparent resistivity curve will be a straight line the ordinate of which is equal to the true resistivity of that medium.

B. Two-layer earth model

The electrode spacing at which the apparent resistivity ρ_a asymptotically approaches the value ρ_2 depends on three factors: on the thickness of the first layer (h_1), value of ρ_2/ρ_1 $(=\mu)$ ratio and on the type of array used to make measurements.

The dependence of the electrode spacing on the thickness of the first layer is fairly oblivious. The larger the thickness of the first layer, the larger the spacing is required for the apparent resistivity to be approximately equal to the resistivity of the second layer. This is true for any array and resistivity ratio. However, for most arrays, including the Schlumberger, Wenner, dipole-equatorial and dipole-axial, if the ration $(\rho_2/\rho_1)>1$, then larger electrode spacing are required for the apparent resistivity to be approximately equal to that when $(\rho_2/\rho_1)<1$.

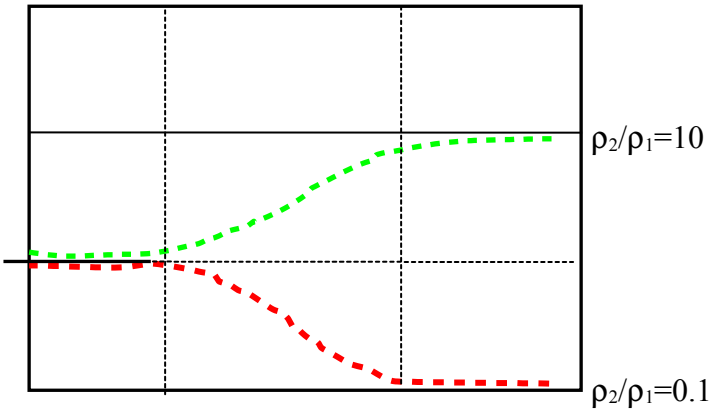

Figure3.4 Possibilities of VES curves over a two layers earth model.

C. Three layer earth model

If the ground is composed of three layers of resistivities ρ_1, ρ_2 and ρ_3 thicknesses of h_1, h_2 and $h_3=\infty$, then the geo-electric section is described according to the relation between the resistivity values.

For a three layers section there are four possible combinations of resistivity values (ρ_1, ρ_2 & ρ_3). These are:

i) $\boldsymbol{\rho_1 > \rho_2 < \rho_3}$ **- *H*** type section (bell shaped)

ii $\boldsymbol{\rho_1 < \rho_2 < \rho_3}$ **- *A*** type section (ascending)

iii) $\boldsymbol{\rho_1 < \rho_2 > \rho_3}$ **- *K*** type section (inverted-up arc)

iv) $\boldsymbol{\rho_1 > \rho_2 > \rho_3}$ **- *Q*** type section (descending)

The use of the letters ***A, Q, H*** and ***K*** to describe a relation between ρ_1, ρ_2, and ρ_3 in the geo-electric section is very convenient and also is used to describe the corresponding sounding curves. Besides, during interpretation it uses to select the proper type of auxiliary master curves.

The interpretation problem for VES data is to use the curve of apparent resistivity versus electrode spacing, plotted from field measurements on bi-log scale graph paper, to obtain the parameters of the geo-electrical section: the layers resistivity and thicknesses. From a given set of layer parameters, it is always possible to compute the apparent resistivity as a function of electrode spacing (the VES curve).

$\rho_a = f(\rho_1, \rho_2, \rho_3 \ldots \rho_i \ldots \rho_n, h_1, h2, h_{3\ldots}, h_{i\ldots}, h_{n-1}, AB/2)$

Unfortunately, for the converse of that problem, it is not generally possible to obtain a unique solution. There is interplay between thickness and resistivity; there may be anisotropy of resistivity in some strata; large differences in geo-electrical section, particularly at depth, produce small differences in apparent resistivity; and accuracy of field measurements is limited by the natural variability of surface soil, rock and by instrument capabilities. As a result, different sections may be electrically equivalent within the practical accuracy limits of the field measurements.

To deal with the problem of ambiguity, VES field curves can be interpreted qualitatively using simple curve shapes, semi-quantitatively with graphical model curves, or quantitatively with computer modeling.

Master Curves

Layer resistivity values can be estimated by matching to a set of master curves calculated assuming a layered Earth, in which layer thickness increases with depth. For two layers, mater curves can be represented on a single plot (Figure 3.5).

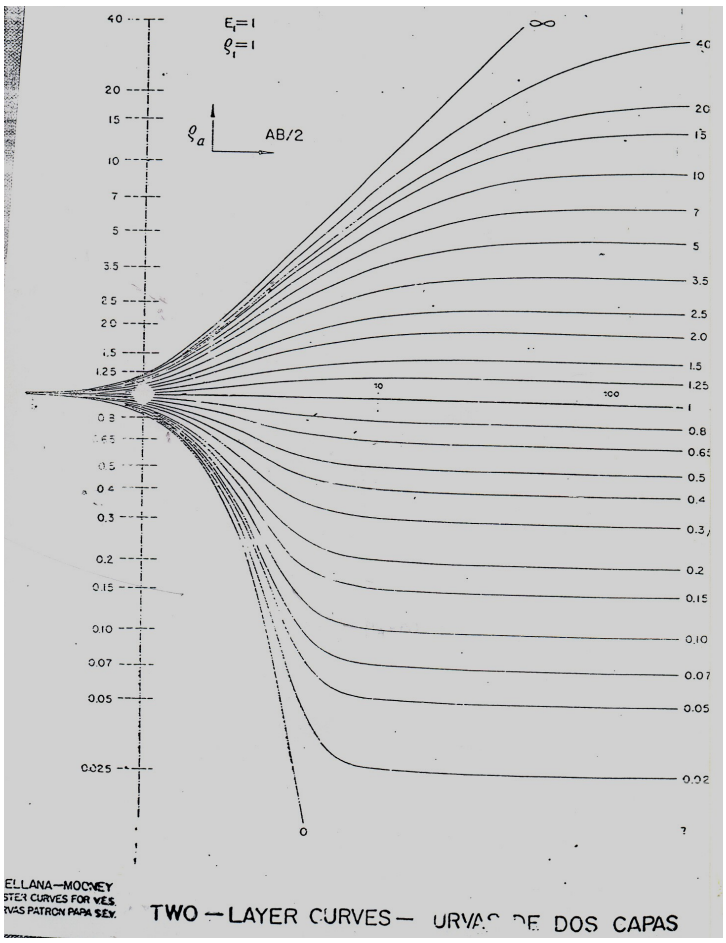

Figure3.5 Master Curve of the two layer Earth model (Telford et.al.)

Master curves: log-log plot with (ρ_a/ρ) on vertical axis and a/h on horizontal (h is depth to Interface)

- Plot smoothed field data on log-log graph transparency.
- Over lay transparency on master curves keeping axes parallel.
- Note electrode spacing on transparency at which (a/h=1) to get interface depth.
- Note electrode spacing on transparency at which to get resistivity of layer 1.

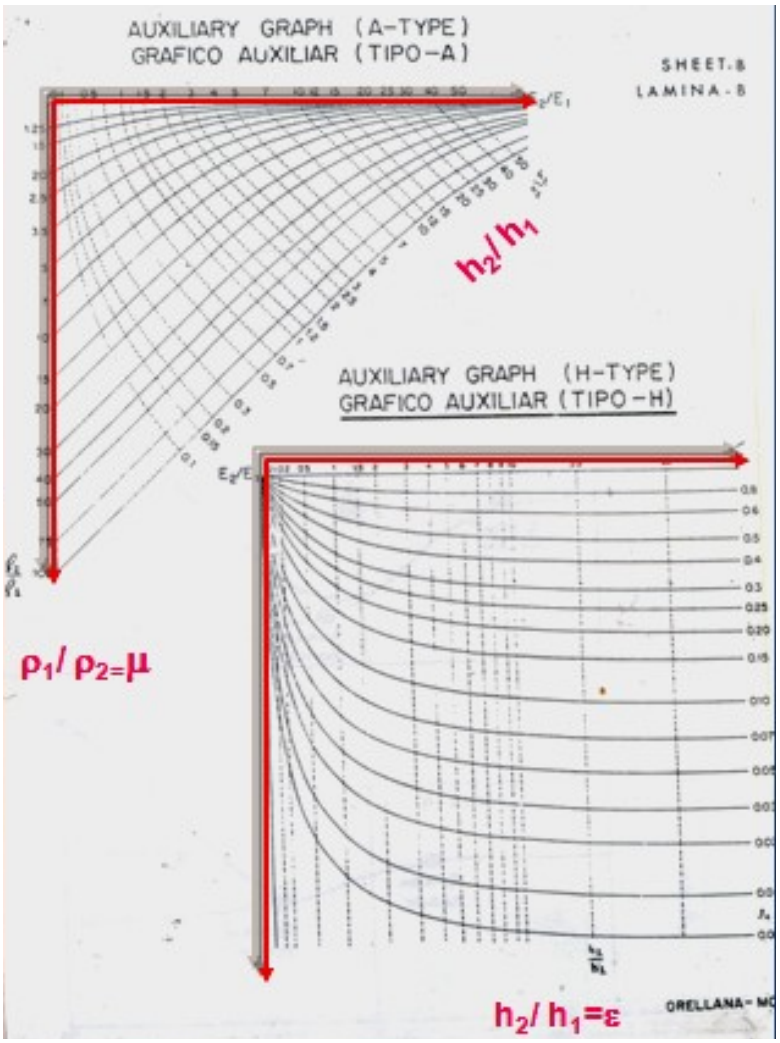

Figure3.6 Auxiliary curves for interpretation of three above layers earth models.

Inversion

Curve matching is also used for three layer models, but book of many more curves.

Recently, computer-based methods have become common:

- Forward modeling with layer thicknesses and resistivity provided by user, and
- Inversion methods where model parameters iteratively estimated from data subject to user supplied constraints. Example (Barker,1992)

Start with model of as many layers as data points and resistivity equal to measured apparent resistivity value.

3.3 MAGNETIC METHOD

Magnetic method is one of the oldest of geophysical exploration techniques used for mineral, groundwater, oil and gas, engineering (locating buried structures and weak zones) and environment applications. The method is a passive potential method. In landslide studies it is useful for mapping of tectonic structures associated with the volcanic basement as they are critical locations for surface ruptures and serve as channel for circulation of subsurface water. Besides, they help to infer morphology of the basement under the thick sediment cover. (Reynolds, 1998).

3.2.2 Basic Theory and Principles

The Earth's large scale magnetic field is superimposed by small scale magnetic anomalies caused by localized magnetized bodies. Magnetization, like density in the gravity method, is the property that characterizes the magnetic moment of rocks per unit volume and this vector quantity is related with the concept of north and South Pole of a magnet (Kirsch, 2009).

Within the vicinity of a bar magnet a magnetic flux is developed which flows from one end of the magnet to the other (Figure 3.7). This flux can be mapped from the directions assumed by a small compass needle suspended within it. The points within the magnet where the flux converges are known as the poles of the magnet. A freely suspended bar magnet similarly aligns in the flux of the Earth's magnetic field. The pole of the magnet which tends to point in the direction of the Earth's North Pole is called positive pole, and this is balanced by the south seeking or negative pole (Kearey et al., 2002).

The force of **F** between two magnetic poles of strengths m_1 and m_2 separated by a distance ***r*** is given by

$$F = \frac{\mu_0 m_1 m_2}{4\Pi \mu_R r^2}$$

Where μ_0 and μ_R are constants corresponding to the magnetic permeability of vacuum and the relative magnetic permeability of the medium separating the poles. The force is attractive if the poles are of different sign and repulsive if they are of like sign.

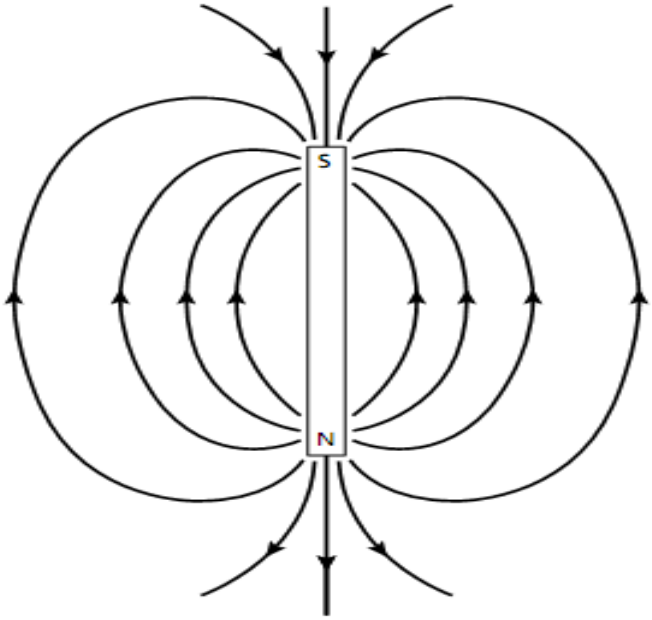

Figure3.7 Magnetic flux surrounding a bar magnet (Kearey et al., 2002).

The magnetic field **B** due to a pole of strength m at a distance r from the pole is defined as the force exerted on unit positive pole at that point

$$B=\frac{\mu_0 m}{4\Pi\mu_R r^2}$$

Magnetic fields can be defined in terms of magnetic potentials. For a single pole of strength m, the potential **V** at a distance r from the pole is given by

$$V=\frac{\mu_0 m}{4\Pi\mu_R r^2}$$

The magnetic field component in any direction is then given by the partial derivative of the potential in that direction.

In the SI system of units, magnetic parameters are defined in terms of the flow of electric current. If a current is passed through a coil consisting of several turns of wire, magnetic flux flows through and around the coil annulus which arises from a magnetizing force **H.** The

magnitude of **H is** proportional to the number of turns in the coil and the strength of the current, and inversely proportional to the length of the wire, so that **H** is expressed in Am-1. The density of the magnetic flux, measured over an area perpendicular to the direction of flow, is known as the magnetic induction of magnetic field **B** of the coil. **B** is proportional to **H** and the constant of proportionality μ is known as the magnetic permeability (Reilly, 1972).

Common magnets exhibit a pair of poles and are therefore referred to as dipoles. The magnetic moment **M** of a dipole with poles of strength ***m*** a distance ***l*** apart is given by

$$M = ml$$

The magnetic moment of a current carrying coil is proportional to the number of turns in the coil, its cross-sectional area and the magnitude of the current.

When a material is placed in a magnetic field it may acquire a magnetization. This phenomenon is referred to as induced magnetization. The intensity of induced magnetization ***J*** of a material is defined as the dipole moment per unit volume of the material

$$\mathrm{J}=\frac{M}{LA}$$

Where ***M*** is the magnetic moment of a sample of length ***L*** and cross-sectional area ***A.*** J_i is consequently expressed in $A^{m^{-1}}$.

The induced intensity of magnetization is proportional to the strength of the magnetizing force H of the inducing field:

$$J_i = kH \tag{3.25}$$

where **k** is the magnetic susceptibility of the material. Since J_i and ***H*** are both measured in $A^{m^{-1}}$, susceptibility is dimensionless in the SI system.

In a vacuum the magnetic field strength *B* and magnetizing force *H* are related by $\boldsymbol{B}=\mu_0 H$ where μ_0 is the permeability of vacuum ($4^{\pi \times 10^{-7} Hm^{-1}}$). Air and water have very similar permeability to μ_0 and so this relationship can be taken to represent the Earth's magnetic field when it is undisturbed by magnetic materials (Kearey et al., 2002).

When a magnetic material is placed in this field, the resulting magnetization gives rise to an additional magnetic field in the region occupied by the material, whose strength is given by $\mu_0 J_i$. Within the body the total magnetic field, or magnetic induction, *B* is given by

$$B = \mu_0 H + \mu_0 J_i \tag{3.26}$$

Substituting equation (3.26)

$$B = \mu_0 H + \mu_0 kH = (1 + k)\mu_0 H = \mu_R \mu_0 H \tag{3.27}$$

where μ_R is a dimensionless constant known as the *relative magnetic permeability*. The magnetic permeability μ is thus equal to the product of the relative permeability and the permeability of vacuum, and has the same dimensions as μ_0. For air and water μ_R is thus close to unity.

3.3.2 Nature of the Geomagnetic Field

As far as exploration geophysics is concerned, the geomagnetic field of the Earth is composed of three parts:

1. The main field or Dipole field B_D, which is produced in the fluid outer core of the earth and accounts for the very large regional variations in the total field intensity and direction.

2. The external magnetic field B_{ext}, which is produced by electric currents in the earth's ionosphere consisting of particles ionized by solar radiation and put into motion by the solar tidal force.

3. The anomalous magnetic field or rock magnetism B_{rm}, which is produced by ferromagnetic minerals and rocks in the earth's crust (Telford et al. 1990). The earth's total magnetic field B_T is given by

$$B_T = B_{ext} + B_D + B_{rm} \tag{3.28}$$

3. 3.3 The Earth's Magnetic Elements

A vector is used to represent the earth's magnetic field at an observation site. At any point on the Earth's surface, the magnetic field **B** has some strength and points in some direction. This vector quantity has a vertical component **Z** and a horizontal component **H** in the direction of the magnetic north. The horizontal component **H** of the magnetic field **B** can be further decomposed into a component **X** in the geographic north direction and a component **Y** in the geographical east direction. The terms which are used to describe the direction of the magnetic field **B** are declination (**D**), the angle between geographic and the magnetic north. The angle of declination is measured positive through east and varies from 0 to 360 degrees, and *inclination* (**I**), the angle between the horizontal **H** and field **B**. Angle of inclination **I** varies from -90^0 to 90^0. These seven magnetic elements are related in the following ways (Figure 3.9).

3.4 Data Reduction and Processing

Data reduction and processing is the series steps taken to remove both signal and spurious noise from the data that are not related to the geology of the site. This process thereby prepares the dataset for interpretation by reducing the data to only contain signal relevant to the task. These steps are summarized below:

i. **Data checking and editing:** involves the removal of spurious noise and spikes from the data that was caused by high tension power cable.

ii. **Diurnal removal:** corrects for the temporal variation of the Earth's main field which was achieved by subtracting the time synchronized signal, recorded at a stationary base magnetometer from the survey data.

iii. **IGRF removal:** removes the strong influence of the Earth's main field. This was achieved by subtracting a calculated of main field using Oasis Montaj from the diurnal corrected survey data.

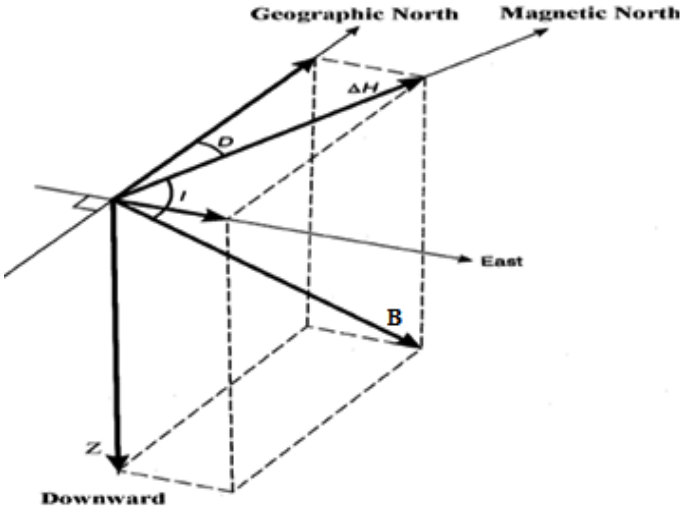

$$H = B\cos i$$

$$Z = B\sin i$$

(3.22)

$$\tan\ i = Z\ /\ H$$

$$\mathrm{X} = \mathrm{H}\cos D$$

$$Y = H\sin D$$

Figure3.8 The earth's magnetic field elements (Reynolds1997).

The processing of the total intensity map revealed a set of processes such as residual map and an alytic signal map. All processed data are mapped and used for qualitative interpretation. The qualitative interpretation for the constructed magnetic maps, aims to get a clear view of the subsurface structures, estimation of the relative depth of the Magnetic anomalies sources.

The quantitative interpretation has been used to determine the depth of shallow subsurface structures (faults and dykes), fractures and contacts of the studied area. The analysis and processing were done by specialized computer program Geosoft (Oasis Montaj).

CHAPTER – 4

4. DATA ACQUISTITING AND PROCESSING

4.1 Vertical Electrical Sounding

4.1.1 Instrumentation and Data Acquisition

Vertical Electrical Sounding (VES) survey was conducted using IRIS Elrec Pro 10 channel with VIP 5000 System and *SARIS* Tetrameter instrument.

The system includes in built quality control tools to aid the operator validity measurements during data acquisition, and displays IP decay curves in real time.

The Elrec Proreciver is designed for use with the VIP series of high power transmitters. The VIP of electrical transmitter is purposely designed for resistivity sounding deep investigations. Fuor VIP systems are available; VIP 3000, VIP 4000, VIP 5000, VIP 10000 which makes the range suitable for use in almost all geological formations. The Elrec Pro automatically synchronizes (and re- synchronizes at each new pulse) with the transmission signal, through the waveform recognition process, ensures high measurement repeatability. To facilitate the identification and orientation of VES points hand held GPS was used. The complete sets for electrical measurements are illustrated in Figure 4.1.

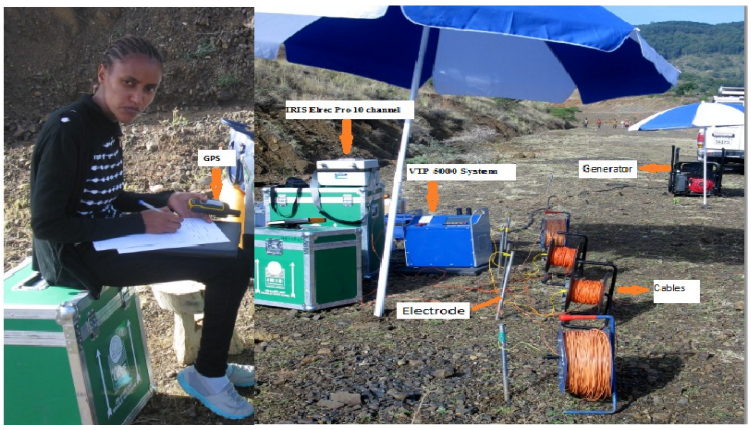

Figure4.1 Electrical field measurements setup

Data were collected along three traverse lines. The two traverses are perpendicular to the slide mass where as the third traverse is across these two traverses. To determine the thickness and area distribution of weathered and fractured rocks in depth in the field totally about 20 VES points with AB/2 separations of about 700 meters were conducted. Symmetrical Schlumberger electrode configuration was used during the survey. These VES points are SW-NE oriented while the third traverse runs nearly perpendicular to the other two traverses as shown in Figure4.3.

4.2.1 Vertical Electrical Sounding Data Processing

The field results of the study are presented in both qualitative and quantitative interpretations.
In the qualitative interpretation the shape of the field curve is observed to get an idea qualitativel y about the number of layers and resistivity values. The vertical electrical sounding data is processed using IP2WIN software. The segmented curves were shifted to the small MN curve points to have precise interpretation. The layer parameter are developed by processing the apparent resistivity data in IP2WIN software with the help of interactive graphics and by changing the model continuously, until a model that best fits to the curve is attained. In the quantitative interpretation method we have pseudo-depth section and geo electric section. Pseudo-depth section map is developed using **Surfer** software from the apparent resistivity collected at field and the distance between the measured points. Even though the pseudo depth section doesn't indicate us exact depth and thickness of the section, it can serve as an initial model to construct geo electrical section. Geo-electrical parameter, i.e. true resistivity and layer

thickness were obtained to make geo-electrical section map. The maps are developed using Surfer. Geo-electric section map is constructed with the help of Surfer software layer parameters generated by **IP2WIN** and **IPI res3** software for the three traverses.

4.2 Magnetic method

4.1.1 Instrumentation and Data acquisition

Magnetic method is employed for subsurface study to outline geological structures that affects the road. The Magnetic data were collected using **GSM-19T Proton Precision Magnetometer** instrument.

Figure4.2 Magnetic data acquisition in the study area

GSM-19T Proton Precision Magnetometer is advanced and proven system offers a range of benefits for different applications. **GSM-19T** Magnetometers has an absolute accuracy of 1nT, resolution, 0.001nT, sensitivity <0.1nT, sampling rate of 2 reading per second up to 60 sec, manually can read coordinates, time, data and reading stored automatically at minimum 2 readings per second interval and it is faster data transfer.

The systems operate on broadly similar principles utilizing proton rich fluids surrounded by an electric coil. A momentary current is applied through the coil, which produces a corresponding

magnetic field that temporarily polarizes the protons. When the current is removed, the protons realign or process into the orientation of the Earth's magnetic field. The precession generates a small electrical current in the surrounding coil, at a frequency directly proportional to the local magnetic field intensity. Gradiometers measure the magnetic field gradient rather than total strength, which allows the removal of background noise (Mariita, 2007).

The surveying was started by establishment of a base station within the study area at a place which is easily accessible and as far as possible from magnetic noise. In addition to the magnetic readings the geographic coordinates of the point at which the readings are taken and the time of reading was recorded using Global Positioning System (GPS). During the midday hours, sunspot activities relatively increases and disturb the readings, due to this reasons all the magnetic data were collected during morning and afternoon to minimize the erroneous data that resulted from solar activity. To cover the area magnetic data were collected randomly within and at the boundary of the study area. Magnetic data were collected about 100 data points with average spacing of 20m along the selected profile lines and 152 data points for the random survey with average spacing of about 40m. Therefore a total of 252 readings were collected during the field survey. At the field survey three magnetic readings were taken for a specific point and then average of this readings were used for the processing and interpretation purpose. The distribution and location of the VES and Magnetic data in the study area is shown below in Figure 4.3.

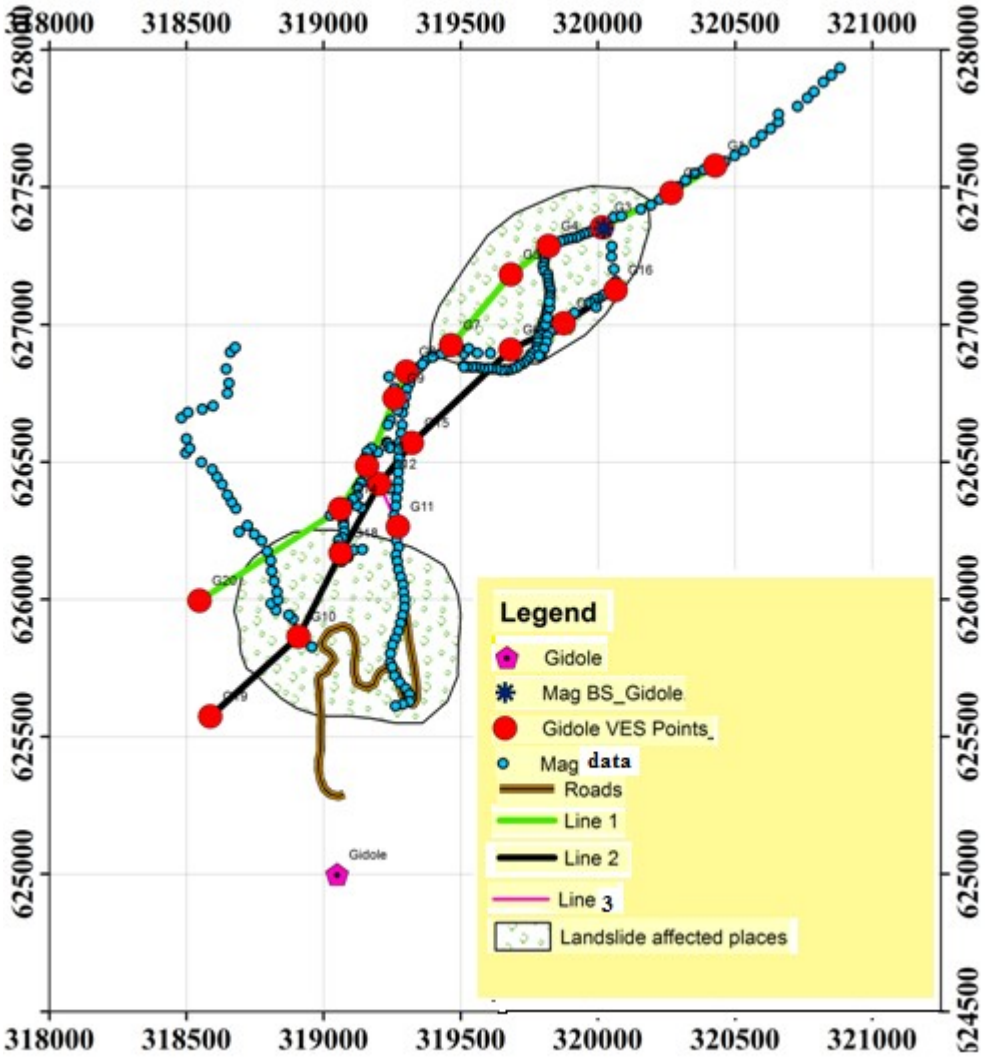

Figure4.3 Location and distribution of VES and Magnetic datas

4.2.2 Magnetic Data Reduction and Processing

Processing of magnetic data includes the correction for daily variations in the Earth's magnetic field and the removal of the geomagnetic correction from our data. For the purpose of diurnal correction the magnetic data collected at field was recorded in Microsoft excel. Using Microsoft excel diurnal correction was done by subtracting the diurnal variation of each reading point from the reading taken by Proton Precision Magnetometer at that specific point. The formula that we used for diurnal correction is :-

$$DC = \left(\frac{BS_2 - BS_1}{T_2 - T_1}\right)(T_r - T_1)$$

Where DC = Dirunal Correction

BS_2 = Reading of Base Station-2

BS_1 = Reading of Base Station-1

T_2 = Observation time of Base Station-2

T_2 = Observation time of Base Station-1

T_2 = Observation time of each measuring points

In addition to the above correction the magnetic data required geomagnetic correction, which is a technique that removes the effect of geomagnetic references field from the survey data. The most accurate method of geomagnetic correction is the use of the International Geomagnetic Reference Field (IGRF) value (Kearey et al., 2002). Therefore, the correction was made using recent (2015) IGRF for the study area is obtained from online IGRF calculator. The IGRF value used for the study area is 34789 nT. And this value is subtracted from the diurnal corrected total field to obtain the anomalies. Finally the total magnetic field anomaly processed to produce anomaly map, Analytical signal map and profile plots using Oasis Montaj of version 6.4.2 and Microsoft excel software. Magnetic anomaly map of the area and profile plots will be discuss on the next chapter.

CHAPTER -5

5. DISCUSSIONS AND INTERPRETATIONS

5.1 General

As discussed in the preceding section, geophysical investigations were made at the landslide affected road, and intended to acquire valuable important information about the overall characteristics of failure zone and associated tectonic features. The results of resistivity sounding survey are presented in the form of separately interpreted curve, apparent resistivity pseudo-sections and for the better qualitative assessments the results are displayed as geo-electric section,. Meanwhile, the magnetic survey results are presented as profile, and contour maps of as total magnetic field anomaly and analytic signal maps with an aim to extract as much information as possible about the subsurface.

5.2 Interpretation of VES data

The measured apparent resistivity values (ρ_a) obtained by the sounding survey were plotted on a log-log scale against the electrode spacing (*AB/2* and after the data were checked and few noisy values were removed the *Ipi2Win* software was used for processing and determine the layer parameters (thickness/depth and resistivity). In the course of processing the program results in best fitting between the actual field data and the synthetic data generated from the model by a least root mean square (RMS) error approach and for all stations the RMS error was found to within 2.5-9.4%. Hence, the determined layer parameters are used to characterize the subsurface formations in light of the survey objectives.

To demonstrate the output the data processing, the results of three sounding stations, i.e., one from each survey profile, are presented here (Figure 5.1), whereas the remaining interpreted curves are as attached as annex (Annex-1). From the interpretation results it became evident that the underlying formations revealed quite distinct resistivity responses that allow to differentiate the roles of the sources in-terms of their characteristics in the process of mass movements.

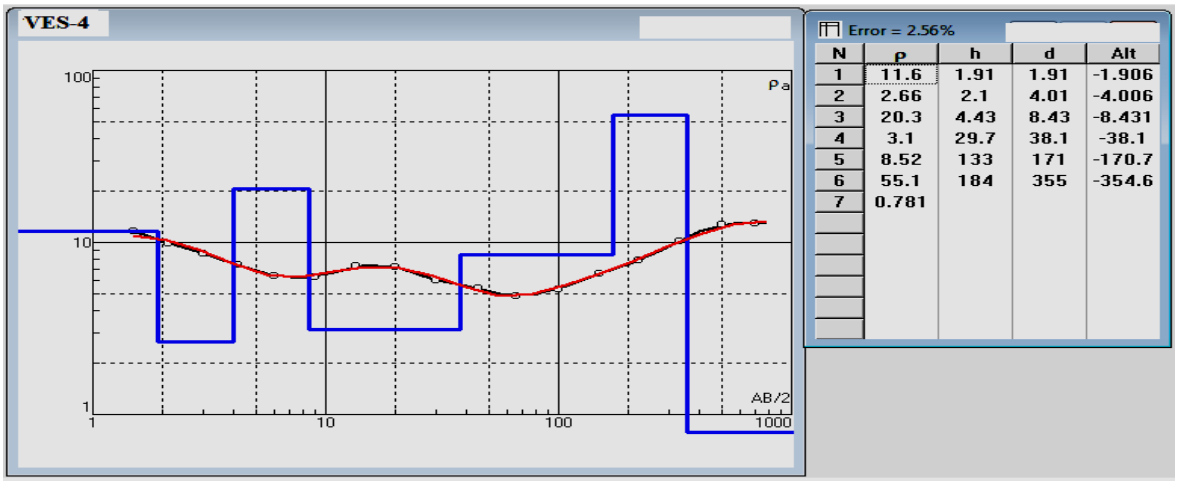

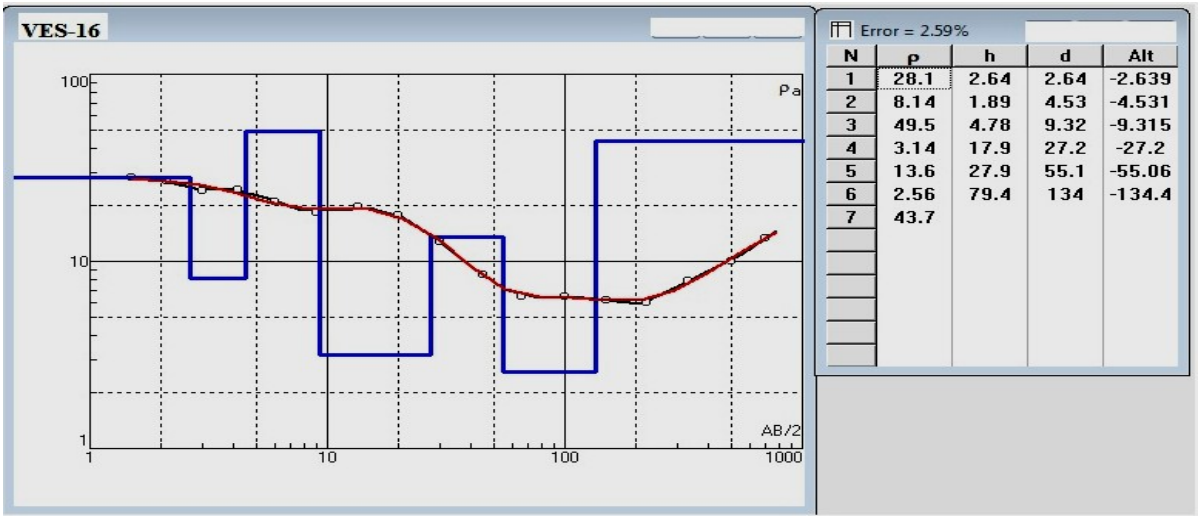

Figure5.1 Samples of interpreted sounding curves for stations VES-4 and VES-16.

Pseudo depth section and Geo-electric Section

Even though pseudo-section are not reflecting the actual depths of anomaly sources, they are good means of displaying the vertical distributions of resistivity values and also can be used as guide when the geo-electric sections are produced. In this case the *SURFER* (Version 10) software was used to plot the presented pseudo-sections and geo-electric section based on which

both qualitative and quantitative interpretations are conducted. In the following sections the results obtained from each survey profile are discussed.

5.2.1 Profile-1

Figure 5.2 displays the pseudo-section along Profile-1, which consists of VES 20, VES 14, VES 13, VES 9, VES 8, VES 7, VES 5, VES 4, VES 3 and VES2 that are aligned from SW to NE direction. Referring to this section one can observe how resistivity values change both laterally and vertically. Somewhere between VES8 and VES5 there is a more resistive feature is possible to note According to this figure, there is a lateral variation of resistivity in the section with high resistivity zones mapped between VES-8 and VES-5, VES-2 has also high resistivity feature is identified at a depth of reached by a spacing of AB/2=200m and above. In the meantime around VES14 and VES4 the resistivity contours show drastic changes. As this pseudo-section displays the raw field data, it is impossible to associate the observed variations with any specific geological features unless the before inverting the data. Nevertheless, the large area of the section has shown relatively small resistivity value (>80 Ωm) and the shallow depth of VES-3 reveals a very small resistive feature..

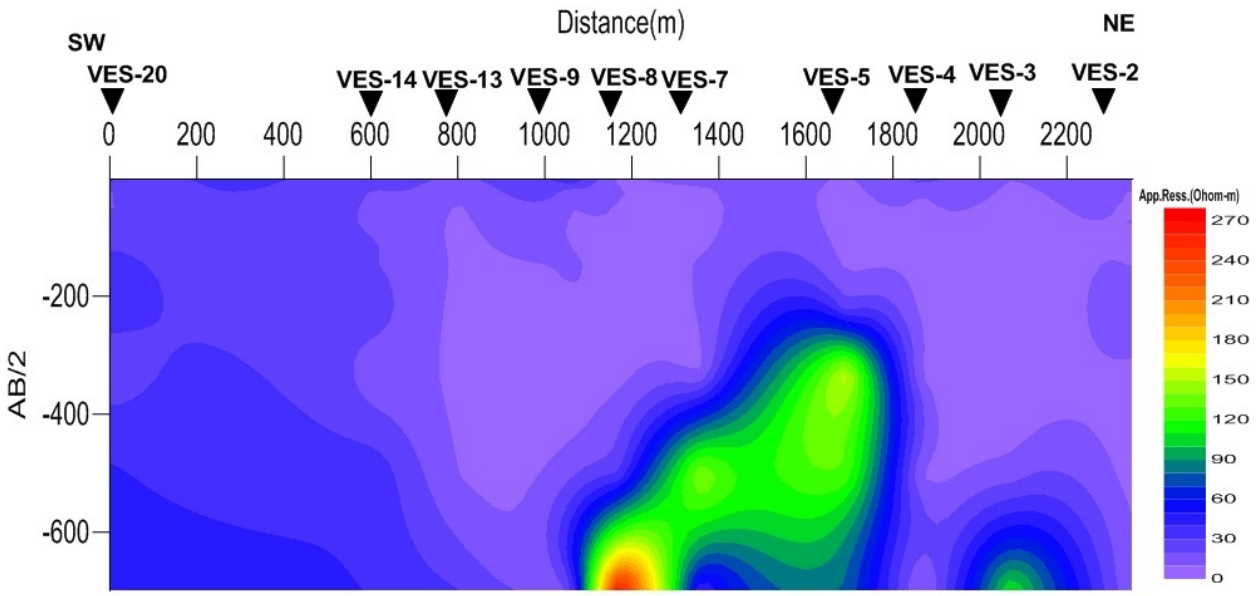

Figure5.2 Pseudo depth section of profile One.

Geo electric Section

The geo-electric section of Profil-1 is displayed in Figure 5.3. This profile included 10 VES stations and has a total length of 2.4 km and oriented in SW-NE direction. Within this profile interval the resistivity values of the inversion result model vary within a wide range, from about one to 10,000 Ohm-m.

Such wide range clearly suggests that the anomaly source bodies are quite distinct in their compositions, grain sizes, moisture contents, degrees of compactions, fracturing and weathering. Generally from the presented section three layers distinct layers are delineated. The uppermost layer with relatively variable resistivity responses (43-77 Ohm-m) and a thickness range of about 0-60m is attributed to be the effect of the upper colluvial deposit consisted of graves, boulders with silt and clay. It is poorly sorted and can easily be removed by external factors such as flood and other anthropogenic factors. This layer is widely distributed on the southern part of the areas covering the elevated topography underlain by volcanic rocks that look relatively intact.

The second and intermediate layer is marked by very low resistivity responses that range between 2 and 32 Ohm-m. Its thickness is quite large that varies from 50 to 150m. Geologically

this conductive layer is assumed to be a product of highly fractured and weathered volcanic (basalts) that has decomposed in to clay sized materials. This layer is also well saturated by groundwater. From the slope instability point of view, this layer whenever gets saturated develops pore water pressure and at some point loses its shear strength and then slides down the slope.

The bottom geo-electrical layer considered as an impermeable hard rock (basalts) is delineated by considerably high resistivity values that are fluctuating from 1400-10,000 Ohm-m. This layer is detected in the depth range from about 150m in the vicinity of VES 20 to about 200m around VES2 and VES3. Geologically, it is associated with fresh-moderately weathered basalt, which at some localities show some discontinuations, possibly fault/fracture zones detected in the vicinity of VES13-VES14 as well as VES3-VES4. At these locations this marking horizon has revealed a drastic thickness changes which may be due to some kind of displacement.

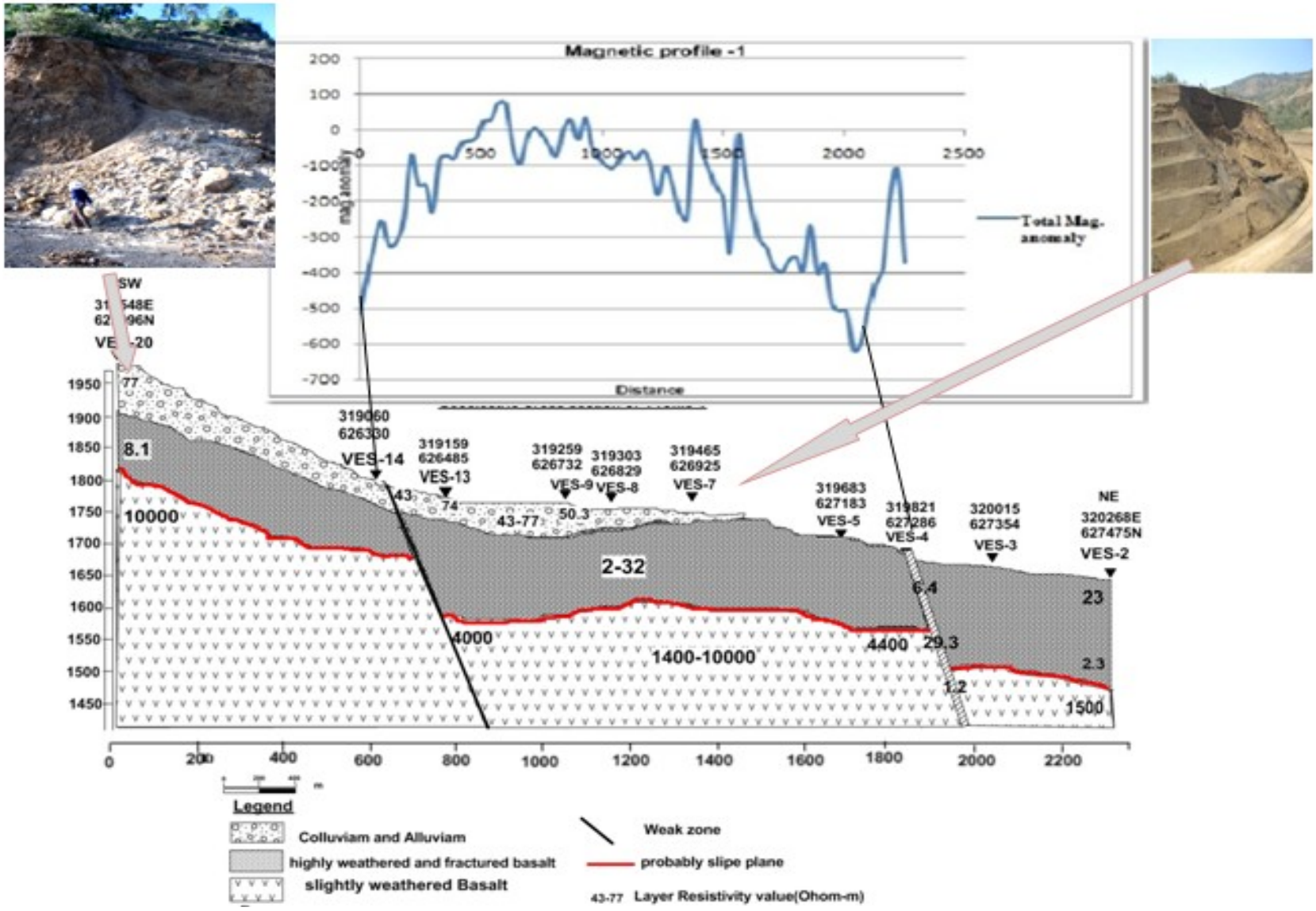

Figure 5.3 Geo-electric section and magnetic plot along profile two.

The resistivity value of these possible structurally disturbed zones was also found very low, which ranges between 1.2 and 20Ωm, which indicates the intensive degree of weathering and fracturing through which water along the weak zones percolates in to or out of the aquifers.

From the presented section is seems easy to outline the possible morphology of the failure surface (slip surface). This inferred slip plane dip towards NE (i.e., towards Lake Chamo direction) and when one looks at the section the degree of inclination of this surface is a bit steep around VES20 and VES13.

The magnetic profile along the geo eclectic section-1starting from VES14 was plotted as shown in the Figure 5.3.we correlate the magnetic profile and the geo eclectic section from VES14-the end because we haven't enough magnetic data match with the VES20 for the reason that the area was canyon. The magnetic profile shows considerable amplitude variation in the magnetic anomaly signatures. The minimum negative peak value is -619.285nT at a distance of about 2040m and the maximum positive peak value is 74.3397nT at a distance of about 540m.There is a good correlation between the magnetic anomaly plot and the geo eclectic section in detecting the weak zones. The magnetic anomaly plot shows a presence of fractured zone at first value and2040m of the profile which are also interpreted same from the geo eclectic section plot with VES14 and VES4.

5.2.2.1 Profile-2

Pseudo depth section

The pseudo-depth section constructed for VES-19, VES- 10, VES-18, VES-11, VES-12, VES-15, VES- 6, VES- 17, VES-16 and VES-1 that lie on the survey traverse line-2 are given in Figure 5.4.

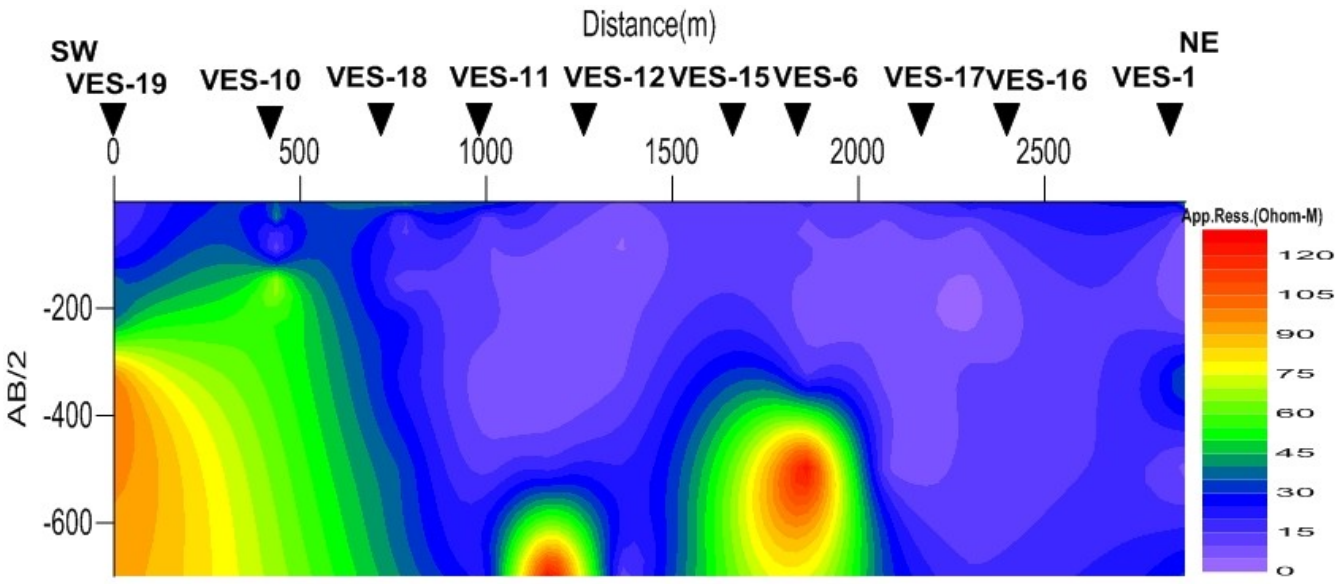

Figure 5.4 Pseudo depth section of profile two

According to this figure, there is a lateral variation in resistivity in the section with prominent high resistivity away from the top zones mapped between VES-15 and VES-6 similarly at VES-19 and VES-10 high resistivity exists near to the top zone. Otherwise, the rest VESs of the section has relatively small resistivity. The resistivity ranges (1 to 35 Ohm-m) of this low resistivity region are indicative of saturated material.

Geo electric Section

Figure 5.5, shows the geo-electric section constructed by correlating the resistivities and thicknesses of the adjacent soundings, which were laid along SW-NE running traverse line of the surveyed area. This geo-electric section has the almost the same value with the previous geo-electric section but there are different traverse lines. These two geo-electric sections are parallel each other located above and below the road affected by landslide problem.

The geo-electric section reveals the presence of three distinct resistivity layers. The topmost layer is characterized by resistivity values 40-60 ohm.-m and having an average thickness of 10m, it may represent loose and fine unconsolidated material possibly colluvial deposit.

The underlying second layer resistivity ranges 2-35 ohm-m and it has an average thickness of 170m. This layer could be related to highly weathered and fractured basalt.

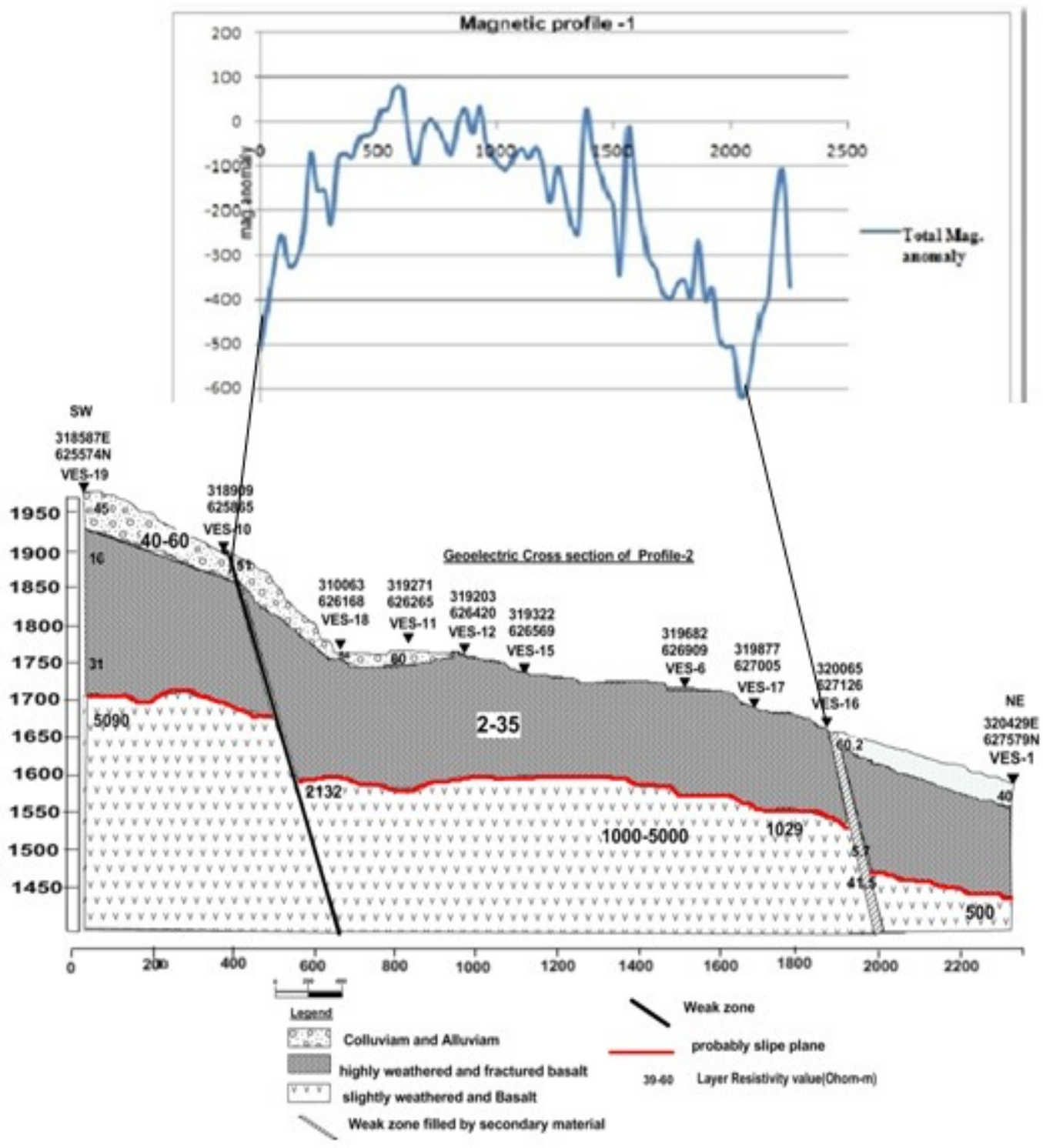

Figure 5.5 Geo-electric section and magnetic plot along profile three.

The third range of resistivity is 500-5000Ωm which may possibly the response of slightly weathered basalt rock. The variation in resistivity along this horizon can be associated to the variation in degree of weathering, intensity of fracturing and geological structures. The left side of the layer being fresh basalt (4000-5000 ohm-m) bounded by slightly-highly weathered basalt (500-2000 ohm-m).This block of fresh basalt rock is characterized by shallower in the southwestern but large depth at northeastern direction of the geo-electric section as shown in Figure 5.5 is displaced by localized structures and similarly, the weathered rock is also dissect by weak zone

Therefore, the weak zone and slope factor may possibly interpret as deriving force for sliding problem at this profile and in other profile as well. And the probably slip plane thickness is about 180m.

5.2.2.1 Profile Three

Pseudo depth section

The pseudo-depth section constructed for VES-11, VES-12 and VES-13 that lie on the Survey traverse line-3 is given in Figure 5.6. According to this figure, there a low resistivity in all VESs in the section.

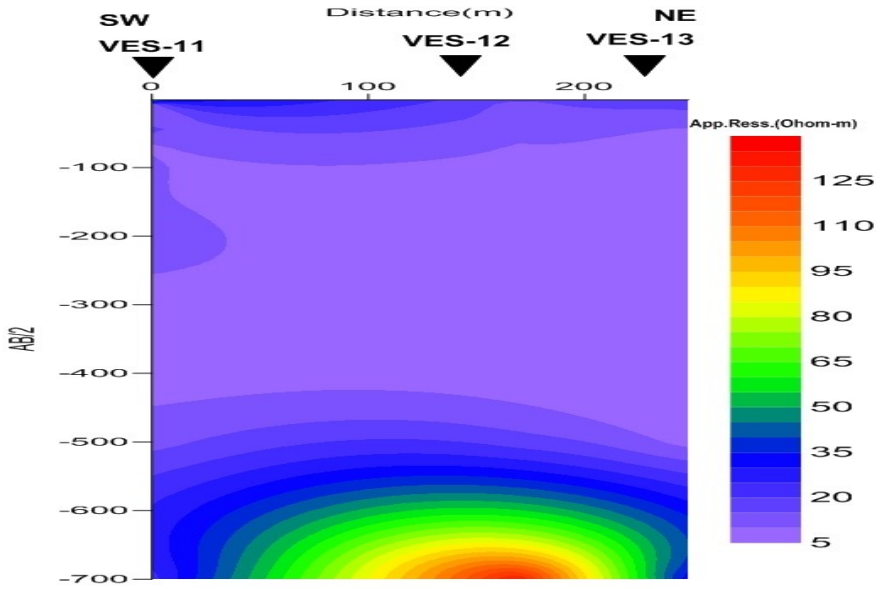

Figure5.6 Pseudo depth section of profile three

The resistivity value is increase with depth at VES-12 but beneath VES-11 andVES13 the resistivity value is low even when the depth increases. This region under the section shows good coverage of the low resistivity.

Geo electric Section

The resulting geo electric section with topography constructed from the interpreted layer parameters of the3 VES lying on this traverse is illustrated on Figure5.7.This third traverse is lies slightly perpendicular to the other two traverses. The interpretation highlights three different resistivity layers.

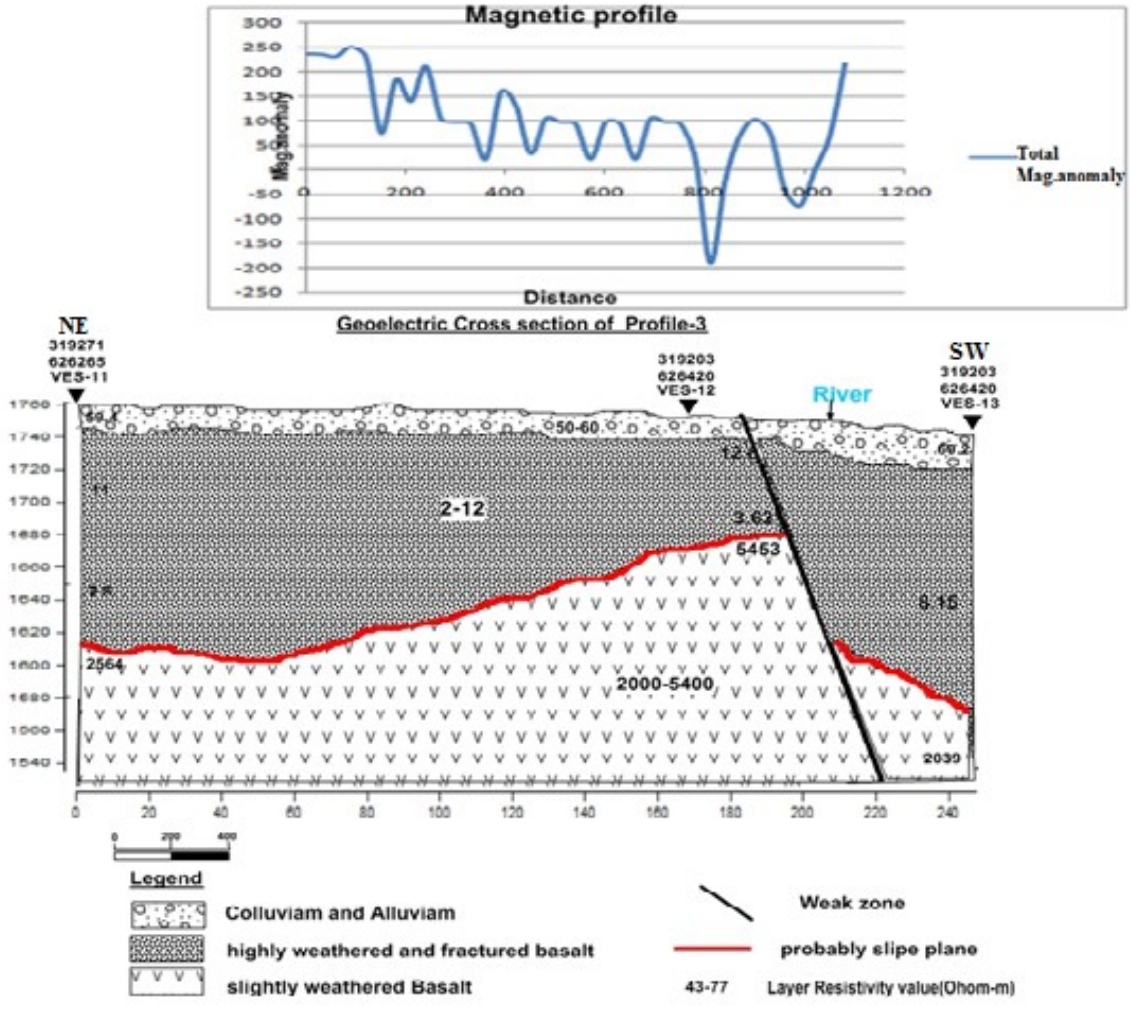

Figure 5.7 Geo-electric section and magnetic plot along profile three

the first layer range resistivity value is varies from 50 to 60 Ωm and average thickness of 20m, these resistivity may responses the alluvial, colluvial and residual soil deposits.

The second geoelectric layer is marked by resistivity values ranging from 2 to12 Ohm m and the thickness variation are from 60- 125m. This layer likely reflects highly fracturedand weathered b asalt. This geo electric layer that corresponds to highly saturated layer.

The third range of resistivity is 5500-2000Ωm which may possibly the response slightly weathered and fractured basalt rock. It lies at a depth of 90m in the vicinity of VES 12, beneath the rest VESs it is relatively deeper (150m).
The thickness of the first and second layer has increased SW and NE direction (VES-11and VES-13) and decreased at the center (VES-12). This is may be due to sliding problem , accumulation of clay soils and slide deposits at this location. The thickness where this range of resistivity is located at this profile becomes greater in comparison to other profiles. This is probably due to the presence of weak zones which are attributed to the intensively weathered and fractured earth materials resulting fragments of rocks.

The magnetic curve and geo electric section Figure 5.7 shows the same pattern in geological structures. The magnetic anomaly plot shows a presence of in geological structures at 810m with minimum negative peak value is -619.285nT 190.399nT of the profile which are also interpreted same from the geo eclectic section plot at VES14.

5.2 Discussions and Interpretation of Magnetics

Magnetic survey is very helpful in identifying geological structures and contact zones of different lithologies. Therefore, the diurnally and IGRF corrected data was processed using different software and subsequently magnetic anomaly map and analytical signal maps were produced which are discussed below.

5.2.1 Magnetic anomaly map

The survey area is displayed in Figure 5.8. From this anomaly map, the subsurface formations have shown relatively erratic anomaly features which are typical for volcanic environment. The magnetic anomaly map has revealed that the northern part of the area is demarked by negative

amplitude but with quite significant amplitude. Besides, this anomalous area shows area shows considerable somewhere in the neighborhood of 627000N latitude. This could be due to a tectonic effect that is inferred at the margin of the cliff just a bit north of Gidole town. The field intensity response is probably due to the result of basaltic rock and covers more in the southwestern which is at the highland part of the study area. The intermediate and low magnetic anomalies zones may be the response of jointed, fractured and weathered basalt and the overlain colluvial deposits as well. It covers hug area almost the northeastern and central parts of the survey area.

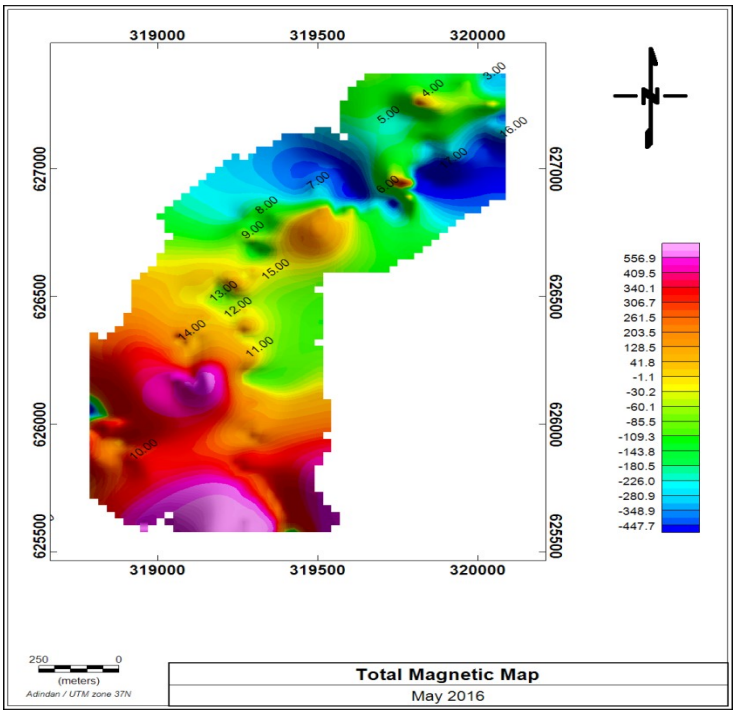

Figure 5.8 Magnetic anomaly map of the study area.

5.2.2 Analytical Signal Map

In order to qualitatively interpret the magnetic data such as estimation of the structural setting and the depth to the magnetic sources, with IGRF Reduction and fine edge enhancement of the subsurface structures using normalized statistics filters we construct an analytical signal map shown in Figure 5.9.

The map shows the responses of anomalous bodies just from the upper part of their sources, calculated for the target area of interest to extract the location of magnetic sources contacts or edges. The analytic signal map is well resolved for shallow anomaly sources but may not be as

such well resolved for deep sources and is good at locating the edges of shallow bodies. The amplitude of the simple analytical signal peaks (maxima) over magnetic contacts does not depend on the directions (inclinations) of magnetization. In addition to these, the map shows zones within the survey area associated with geological contacts According to analytic signal map it is evident that the study area is dominated by structural bodies (fracture zone and faults). . This analytical map shows that the anomalous bodies are in northeastern part of the survey area.

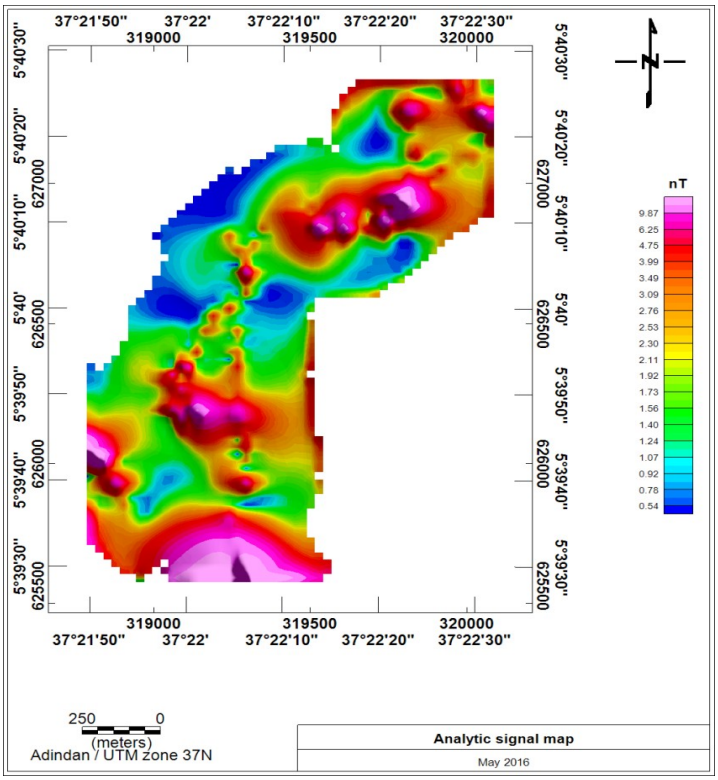

Figure 5.9 Analytical signal map of the study area

CHAPTER-SIX

6. CONCLUSION AND RECOMMENDATION

6.1 Conclusions

Integrated geophysical investigations have been conducted to examine the landslide problem in Welaite Kebele, near Gidole Town, SNNP. Vertical Electrical Sounding and Magnetic methods were applied to map the subsurface features in relation to the landslide problem that hampered the construction of the Arbaminch–Gidole asphalt road, which remained abandoned.

Based on the results of interpretation the following conclusions are forwarded:

i) In the study area three major subsurface layers and structure weak zones are delineated and are characterized based on their physical properties. The lithologies underlying the study area have shown resistivity responses varying within a wide range (1-10,000 ohm-m). The top unconsolidated colluvial deposit (4-77ohm-m) with a maximum thickness of 60m is underlain by a thick bed delineated by low resistivity responses, 2.5-32 Ohm-m. This high conductive nature of layer is clear indication of its high degree of saturation. The bottom layer is the most resistive one with responses between 1000 and 10000 Ohm-m that clearly represent the effect of a fresh-moderately weathered basalt that is widely distributed in the area. This layer serves as an impermeable bedrock above which groundwater can be accumulated.

ii) Based on the analyses of the survey data, the most probable failure surface is inferred to occur in the depth range of 175-250 m. From the results the inferred rapture surface is delineated at the contact between the second and the third layers. Its morphology is relatively simple, with a general dipping trend towards NE.

iii) Both the resistivity and magnetic survey data have, more or less, equally suggested the possible presence of structurally disturbed zones around VES14 and VES4. These features might have considerable contributions in aggravating the landmass movement occurred in the area.

iv) The main triggering factors for landslide problem in the area are heavy rainfall and subsequent rising of the groundwater table, the presence of weak (unconsolidated and

highly saturated) geological formations underlying the inclined topography as well as the presence of tectonic features Therefore, construction of road and other infrastructures require careful consideration of the detail physical properties of the underlying layer in the site.

6.2 Recommendations

On the basis of the outcomes of this study the following thoughts are recommended, in relation to the land sliding problem in the study area:

i) The geophysical investigations have revealed that sub-surface under the area where the route is aligned (passes through) is highly susceptible to active landslides. Therefore, before entering in to the development of such infrastructures, the specific conditions have to be assessed in order to ensure their safety and sustainability. However, the acquired information suggests that the physical property of the foundation materials doesn't seem suitable to put heavy civil engineering structures, including asphalt road.

ii) The main road is highly affected by landslide problem; from the geophysical results the subsurface condition of the abandoned road has significant thickness of colluvial and alluvial deposits, weathered/decomposed and fractured basalts and weak zones. Therefore, even if the abandoned route will not be used as per the initial plan, the area it encompasses needs due attention for special remedial measures to prevent it from further damages.

iii) From field observations the occurrence of groundwater, springs and seepages have noted to have significant role in aggravating the sliding problem over the entire study area, especially in the rainy season as rate of discharge increases. Therefore, proper surface drainage system should be utilized to reduce the intensity of sliding phenomena that highly affected not only the built structures, but also the natural environment.

iv) Because of the shortage of time and extended heavy rain times it was not possible to continue the geophysical surveys applying seismic refraction and gravity methods. Therefore, the current study was limited to VES and Magnetic investigations only. To compliment these results the mentioned methods should be applied and integrated interpretations should be conducted.

7. REFERENCES

Asmelash Abay (2012).Remote Sensing & GIS-based Mapping on Landslide Phenomena and Landslide Susceptibility Evaluation of Debresina area, Ethiopia: PhD Thesis. Università degli Studi di Cagliari,Itali.

Anbalagan,R., and Singh, B. (1996). Landslide hazard and risk assessment mapping of mountainous terrains a case study from Kumaun Himalaya, India. *Engineering Geology* **43**(4): 237-246pp.

Barker,(1992).Cited on Lecture notes on Electrical and electromagnetic.exploration (GPH221) [http://www.aalamri.com/index/download/id/78 /lang/ar, accessed on Mar 24, 2015.]

Bichler, A., Bobrowsky, P., Best M., Douma, M., Hunter, J., Calvert T. and Burns R. (2004). Three-dimensional mapping of a landslide using a multi-geophysical approach: the Quesnel Forks landslide, *Landslides* **1** (1), 29-40pp.

Ceri, J. (1972). The Geology of Chencha district, EIGS, unpublished report, p 10, (map 1:100000).

Cruden, D.M., and Varnes D.J. (1996). "Landslide types and processes". In: Turner, A.K. and Shuster, R.L. (eds) (1996).Landslides investigation and mitigation.Transportation Research Board, Washington, D.C., US National Research Council. *Special report* **247**:36- 75pp.

Davidson, A., and Rex, D.C. (1980).Age of volcanism and rifting in southern Ethiopia:*Nature*,**283**,657-658pp.

Davidson, A. (1983). The Omo River Project, Ministry of Mines and Energy, (EIGS), 89pp. (1:250000 and 1:500000 geological maps).

Ebinger, C.J.,Yemane, T., Woldegebriel, G., and Aronson,J. (1993). Late Eocene-recent volcanism and faulting in the southern Main Ethiopian Rift system: *Geological Society of LOndaon Journal*, **150**.

Ebinger, C., and Sleep, N. (1998). Cenozoic magmatism throughout East African resulting from impact of a single plum:*Nature*,**395**,788-791pp.

EIGS. (1994). Engineering geophysical investigation along proposed alternative route, Blue Nile Gorge. EIGS. Ethiopia. Unpublished report.

EIGS. (1998). Investigation of slope instability problem in the Blue Nile gorge. EIGS. Ethiopia.

EIGS. (1999). Integrated engineering geological and geophysical investigation for Landslides study in Bonga town and its surrounding. EIGS. Ethiopia. Unpublished report.

EIGS. (2014). Summary Report for Landslide Investigation in Gidole Area, Unpublished technical report.

Gebreselassie Gebreanenia,(2013). Investigations of landslide problem using geophysical techniques around Debresina–armania main road: in Tarmaber woreda, northern Shewa zone, Ethiopia, Unpublished MSc thesis.

Göktürkler, G., Ç. Balkaya, and Z. Erhan, (2008). Geophysical investigation of a landslide: The Altındağ landslide site, İzmir (western Turkey): *Journal of Applied Geophysics* **65**, 84–96pp.

Habberjam,G.M.(1979).Apparent Resistivity and the Use of Square Array Techniques..Gebrüder Borntraeger, Berlin. **34**, 780-784pp.

Hagedron, S. (2014).land slide investigation using seismic refraction techniques.

Heather, L. (1999). Electrical Imaging: A method for identifying potential collapse and other karsts feature near roadways. Science Applications InternationalCooperation, Middletown, Pennsylvania.

Kearey, P., Brooks M., and Hill, L. (2002). *An Introduction to Geophysical Exploration*. Third edition. Blackwell Science Ltd, UK, 183-197pp.

Kinfe Woldearegay, (2005). Rainfall-triggered landslides in the northern highlands of Ethiopia: Characterization, GIS-based Prediction and Mitigation. PhD Thesis. Facul. of Civil Eng. Graz Univ. of Techno. 176pp

Kirsch, R.(2009). Groundwater Geophysics. 2nd Edition. Hamburger Chaussee, Germany, 275-286pp

Loke, M.H. (1999). Electrical imaging surveys for environmental and Engineering studies. A practical guide to 2-D and 3-D surveys, Penang, Malaysia.

Loke, M. H. (2001). Electrical Imagine Survey for Environmental and Engineering Studies: A practical guide to 2D and 3D surveys.

Lulseged Ayalew. (1999). The effect of seasonal rainfall on landslides in the highlands of Ethiopia. *Bulletin of Engineering Geology and the Environment* ***58***(1), 9-19pp.

Mariita, N.O. (2007). The Magnetic Method. Presented at Short Course II on surface Exploration for Geothermal Resources, Organized by UNU-GTP and KenGen, at Lake Navivash,Kenya.2-17 pp.

Reilly,W.I. (1972). Use of International System of Units in Geophysical Publications. N.Z.J. Geol. *Geophysics* **15**; 148-58pp.

Reynolds, J. M. (1997). An *Introduction to Applied and Environmental Geophysics*. John Wiley and Sons. limited, England, UK, 160pp.

Reynolds, J.M. (1998). *An Introduction to Applied and Environmental Geophysics*, John Wiley and Sons limited, England, UK.

Robert, D.H and William, D.K. (1981) .An Introduction to Geotechnical engineering, Prentice Hall, Englewood Cliffs, New Jersey 07632, USA, pp 746.

Telford, W.M., Geldart L.P. and Sheriff R.E. (1990). *Applied Geophysics*. Cambridge university press, New York, USA **2**, 760 pp.

Tigistu Haile. (2014). Electrical methods of prospect, unpublished teaching materials.

Varnes D.J. (1978).Slope movement types and processes. In: Schuster RL, Krizek RJ (eds.), Landslides: Analysis & Control. Natio. Aca. of Sci, Transport. Resear. Board, W.DC, Special Rept.**176**,11-35pp.

Woldegebriel, G., Yemane, T., Suwa, G., and Asfaw,B. (1991).Age of volcanism and rifting in Brji –Soyoma area ,southern Mian Ethiopia Rift :geo and bio-chronologicdata:*Journalof African Earth Sience*,**13**.

Zanettin, B. and Justin V. E. (1978). The evolution of the Chencha escarpment and Ganjuil graben (Lake Abaya in the Southern Ethiopian Rift). *N.Jb.Geol.Paaont.Mh* **8**,473 – 490pp.

Zohdy,A.A.R.(1980). Application of Surface Geophysics to Groundwater Investigations: Electrical methods, techniques of water resource investigations of the U.S. geol. Surv.

Declaration

I, the under signed, certify that the work is entirely my own and not of any other person and that all sources of materials used for the thesis have been duly acknowledged.

Name: Kisanet Abera

Signature ……..

The Thesis has been submitted for examination with my approval as university advisor.

Name: Dr. Getnet Mewa

Signature ……..

Place and date of submission: School of graduate studies

Addis Ababa University

Addis Ababa

JUNE, 2016

Annex

Annex -1 Interpreted VES curves of the each sounding points

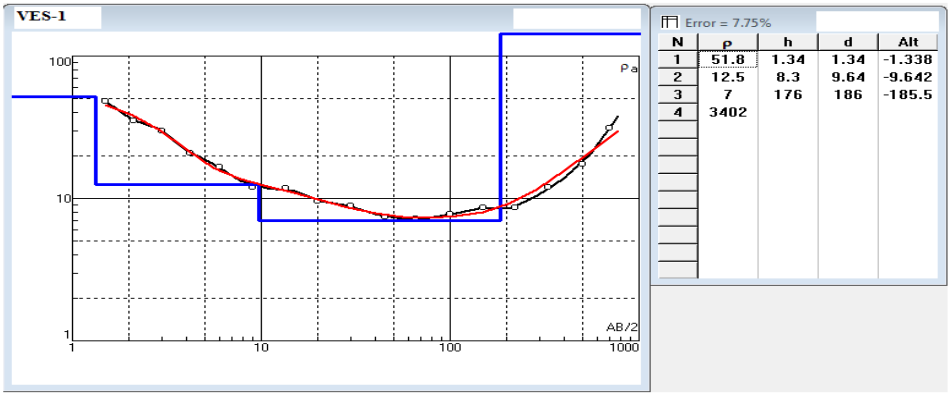

N	ρ	h	d	Alt
1	51.8	1.34	1.34	-1.338
2	12.5	8.3	9.64	-9.642
3	7	176	186	-185.5
4	3402			

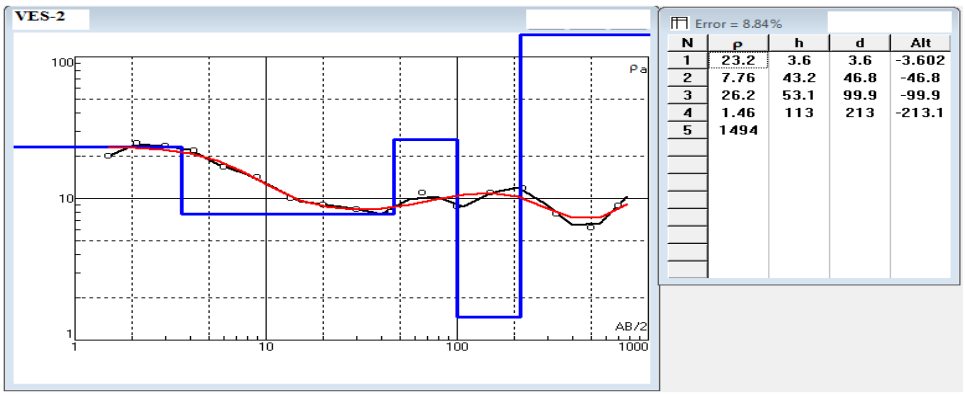

Error = 8.84%

N	ρ	h	d	Alt
1	23.2	3.6	3.6	-3.602
2	7.76	43.2	46.8	-46.8
3	26.2	53.1	99.9	-99.9
4	1.46	113	213	-213.1
5	1494			

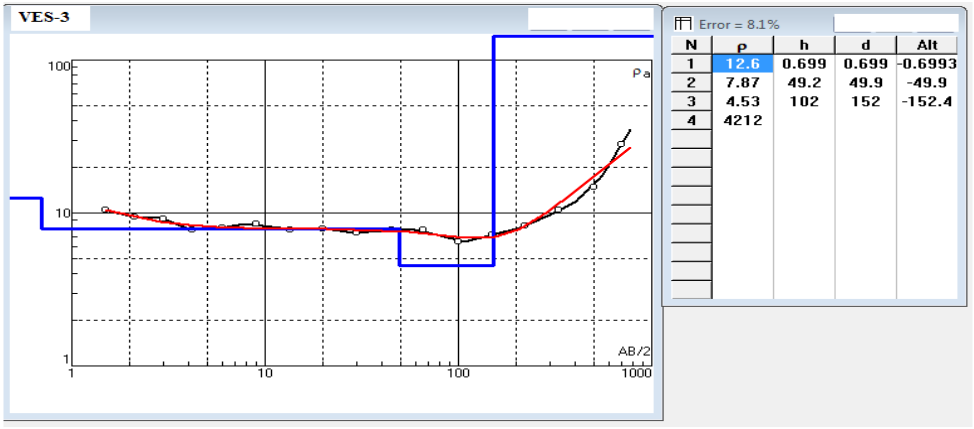

Error = 8.1%

N	ρ	h	d	Alt
1	12.6	0.699	0.699	-0.6993
2	7.87	49.2	49.9	-49.9
3	4.53	102	152	-152.4
4	4212			

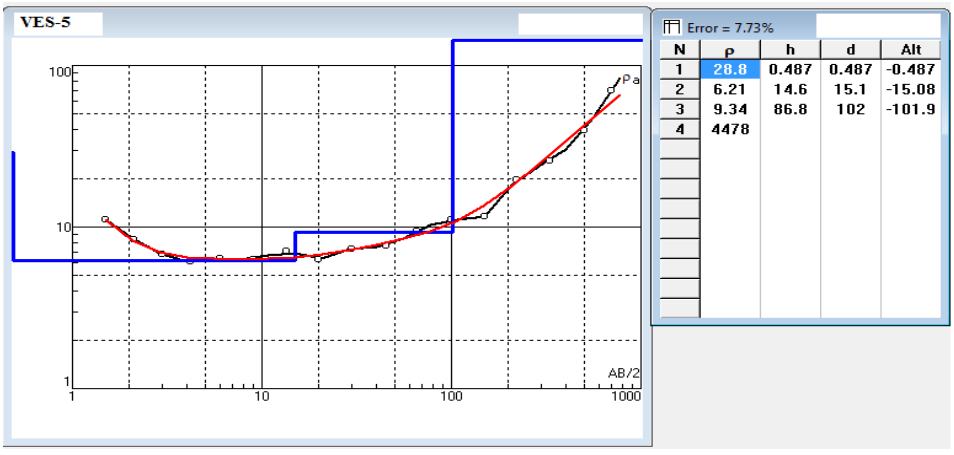

Error = 7.73%

N	ρ	h	d	Alt
1	28.8	0.487	0.487	-0.487
2	6.21	14.6	15.1	-15.08
3	9.34	86.8	102	-101.9
4	4478			

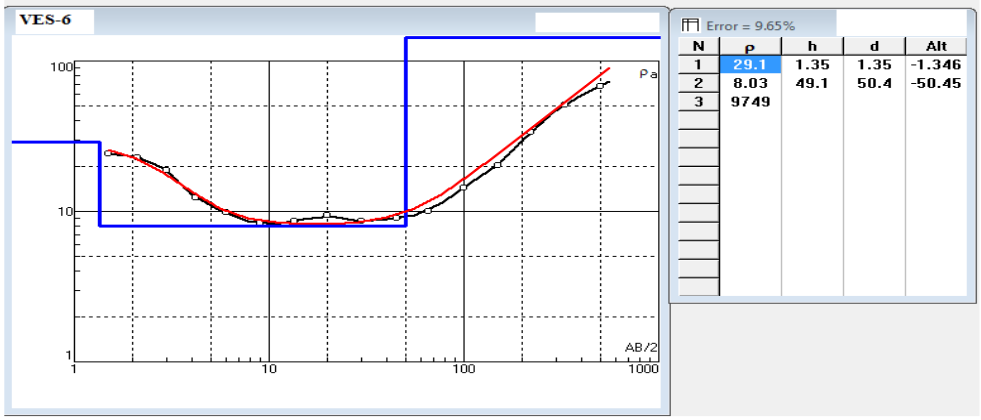
VES-6
Error = 9.65%
N ρ h d Alt
1 29.1 1.35 1.35 -1.346
2 8.03 49.1 50.4 -50.45
3 9749
ρa
AB/2
100
10
1
1
10
100
1000

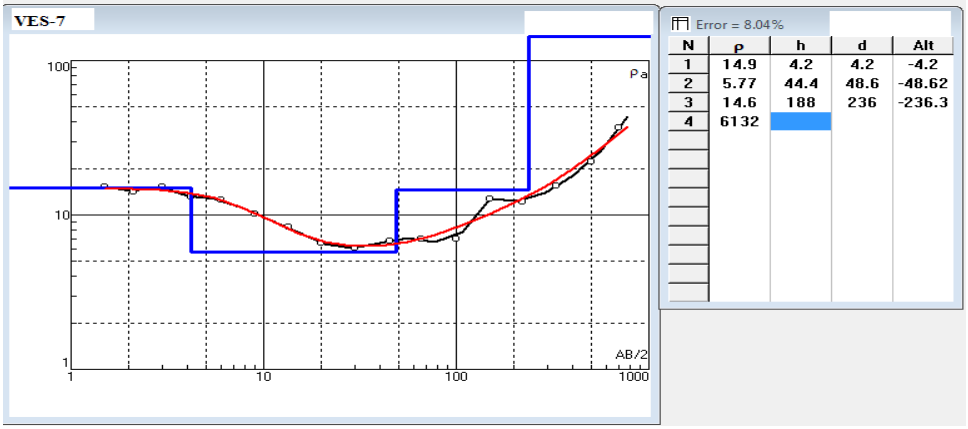
VES-7
Error = 8.04%
N ρ h d Alt
1 14.9 4.2 4.2 -4.2
2 5.77 44.4 48.6 -48.62
3 14.6 188 236 -236.3
4 6132
ρa
AB/2
100
10
1
1
10
100
1000

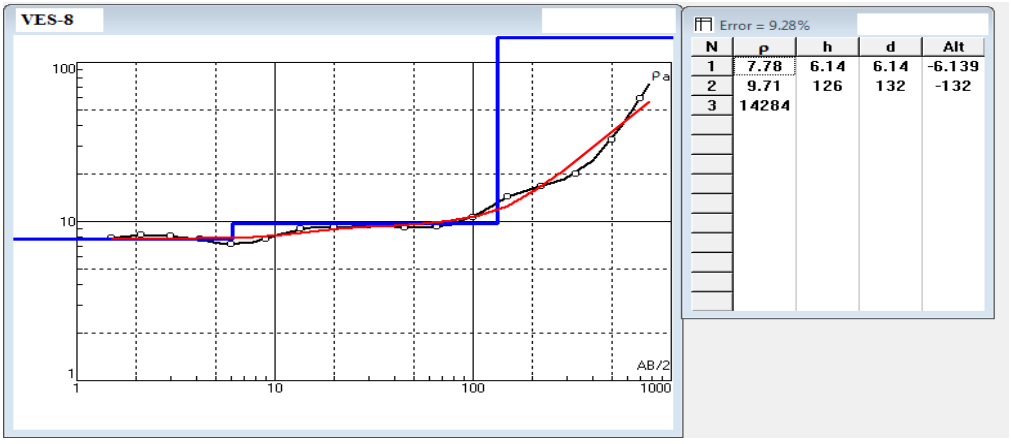
VES-8
Error = 9.28%
N ρ h d Alt
1 7.78 6.14 6.14 -6.139
2 9.71 126 132 -132
3 14284
ρa
AB/2
100
10
1
1
10
100
1000

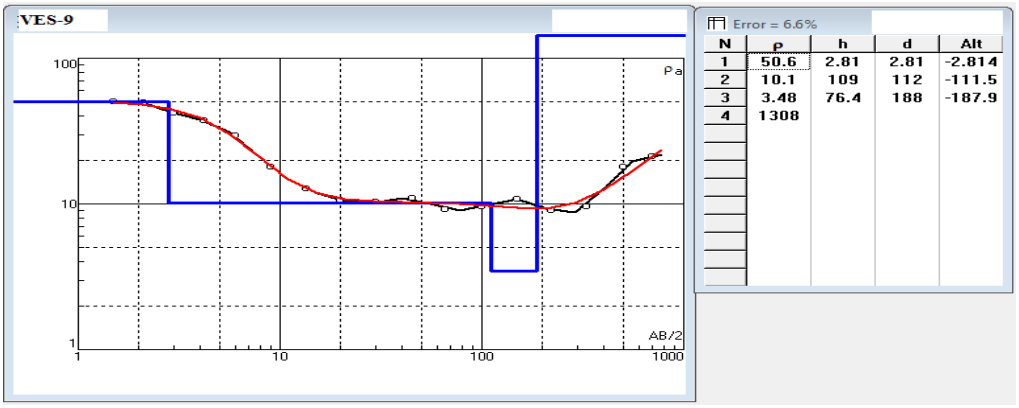

Error = 6.6%

N	ρ	h	d	Alt
1	50.6	2.81	2.81	-2.814
2	10.1	109	112	-111.5
3	3.48	76.4	188	-187.9
4	1308			

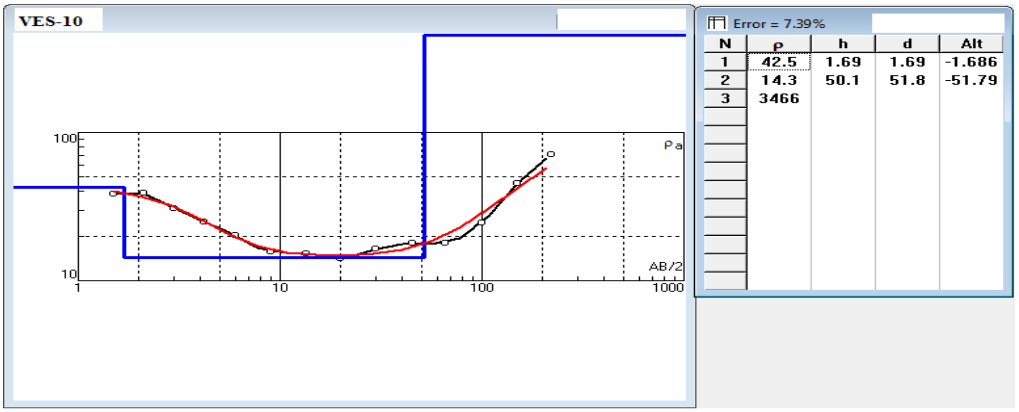

Error = 7.39%

N	ρ	h	d	Alt
1	42.5	1.69	1.69	-1.686
2	14.3	50.1	51.8	-51.79
3	3466			

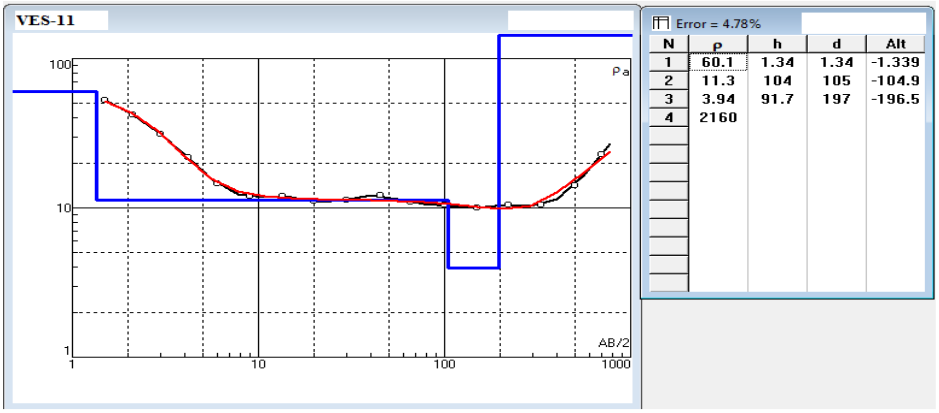

Error = 4.78%

N	ρ	h	d	Alt
1	60.1	1.34	1.34	-1.339
2	11.3	104	105	-104.9
3	3.94	91.7	197	-196.5
4	2160			

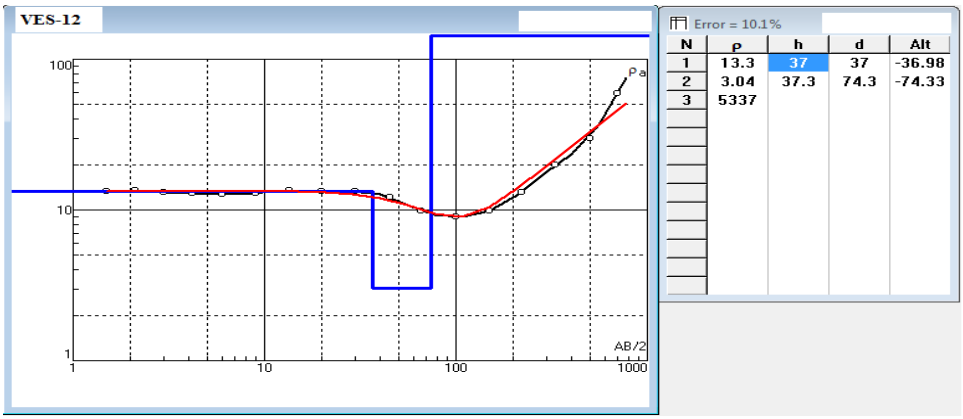

Error = 10.1%

N	ρ	h	d	Alt
1	13.3	37	37	-36.98
2	3.04	37.3	74.3	-74.33
3	5337			

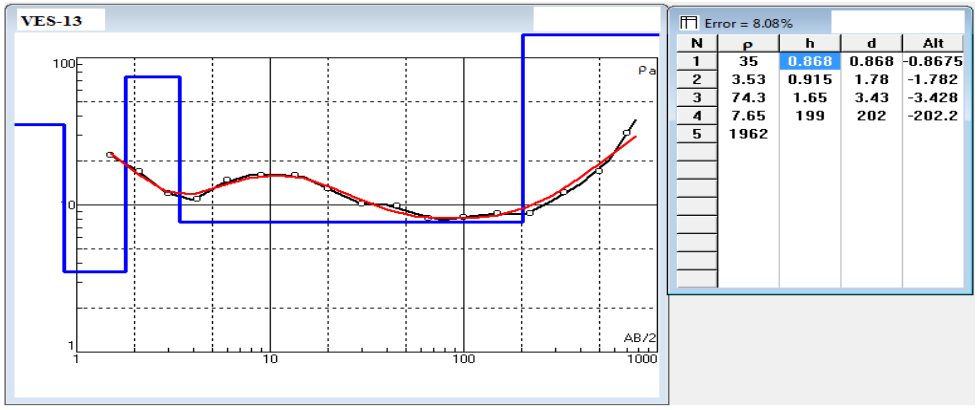

Error = 8.08%

N	ρ	h	d	Alt
1	35	0.868	0.868	-0.8675
2	3.53	0.915	1.78	-1.782
3	74.3	1.65	3.43	-3.428
4	7.65	199	202	-202.2
5	1962			

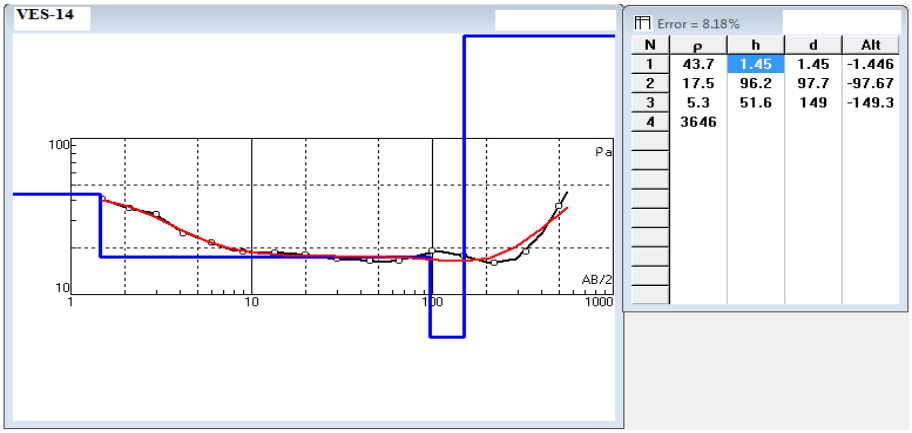

Error = 8.18%

N	ρ	h	d	Alt
1	43.7	1.45	1.45	-1.446
2	17.5	96.2	97.7	-97.67
3	5.3	51.6	149	-149.3
4	3646			

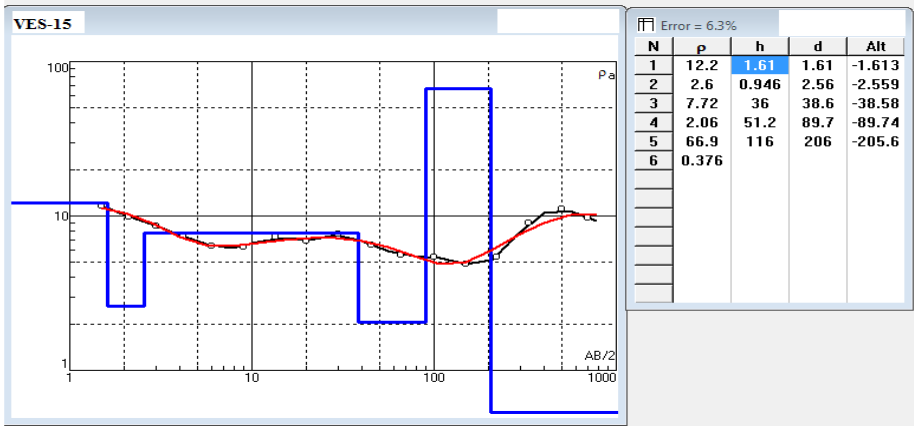
VES-15
Error = 6.3%
N ρ h d Alt
1 12.2 1.61 1.61 -1.613
2 2.6 0.946 2.56 -2.559
3 7.72 36 38.6 -38.58
4 2.06 51.2 89.7 -89.74
5 66.9 116 206 -205.6
6 0.376
ρa
AB/2
100
10
1
1
10
100
1000

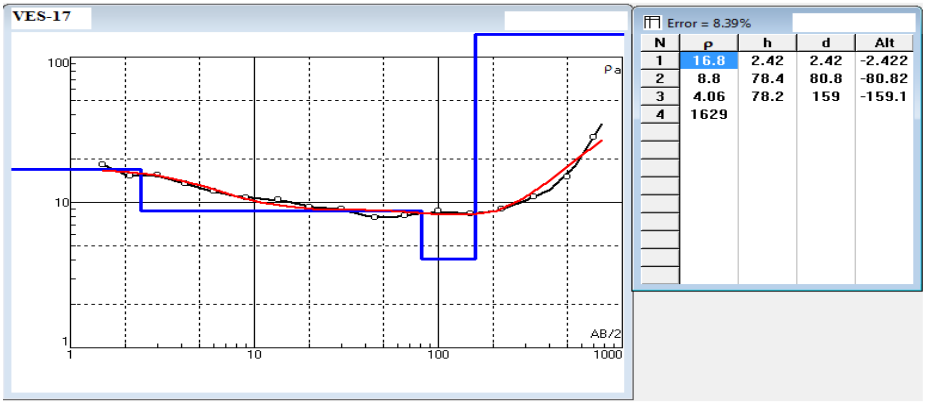
VES-17
Error = 8.39%
N ρ h d Alt
1 16.8 2.42 2.42 -2.422
2 8.8 78.4 80.8 -80.82
3 4.06 78.2 159 -159.1
4 1629
ρa
AB/2
100
10
1
1
10
100
1000

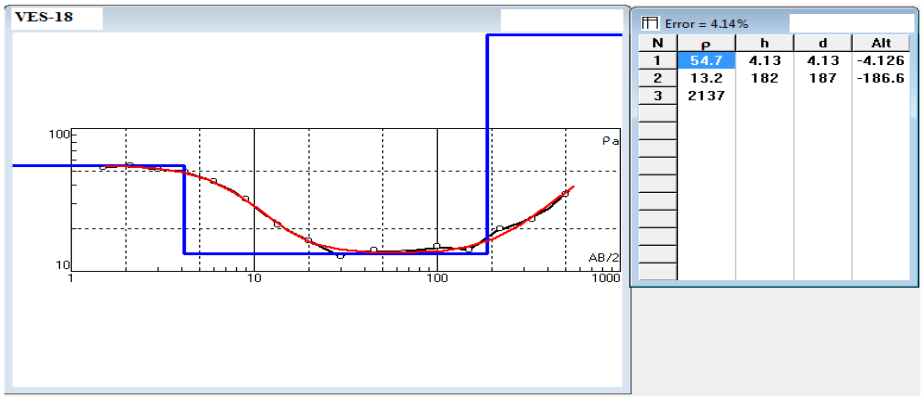
VES-18
Error = 4.14%
N ρ h d Alt
1 54.7 4.13 4.13 -4.126
2 13.2 182 187 -186.6
3 2137
ρa
AB/2
100
10
1
10
100
1000

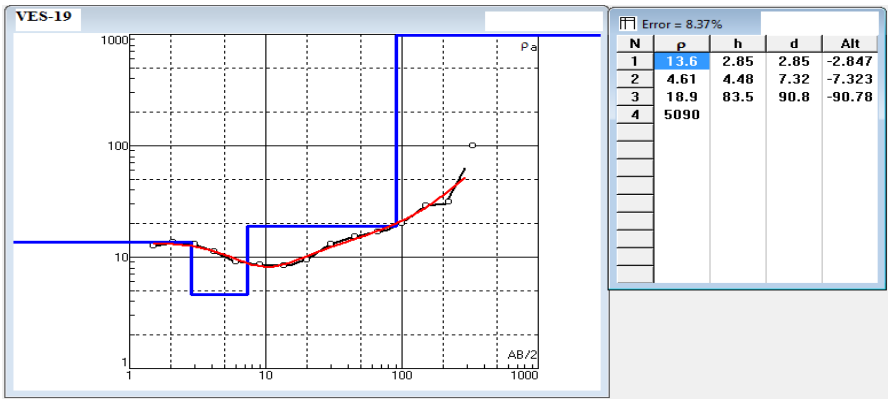

Error = 8.37%

N	ρ	h	d	Alt
1	13.6	2.85	2.85	-2.847
2	4.61	4.48	7.32	-7.323
3	18.9	83.5	90.8	-90.78
4	5090			

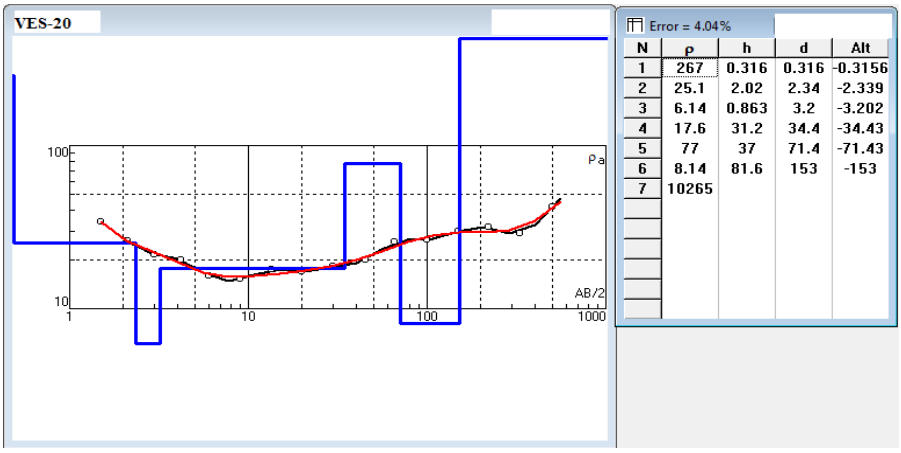

Error = 4.04%

N	ρ	h	d	Alt
1	267	0.316	0.316	-0.3156
2	25.1	2.02	2.34	-2.339
3	6.14	0.863	3.2	-3.202
4	17.6	31.2	34.4	-34.43
5	77	37	71.4	-71.43
6	8.14	81.6	153	-153
7	10265			

Annex-2: Photographs showing landslide effects on the study area: